EUROPEAN ORGANIZATION FOR NUCLEAR RESEARCH (CERN)

CERN-EP-2025-017
2025/11/07

CMS-SUS-23-001

Search for top squarks in final states with many light-flavor jets and 0, 1, or 2 charged leptons in proton-proton collisions at $\sqrt{s} = 13\,\text{TeV}$

The CMS Collaboration*

Abstract

Several new physics models including versions of supersymmetry (SUSY) characterized by R-parity violation (RPV) or with additional hidden sectors predict the production of events with top quarks, low missing transverse momentum, and many additional quarks or gluons. The results of a search for top squarks decaying to two top quarks and six additional light-flavor quarks or gluons are reported. The search employs a novel machine learning method for background estimation from control samples in data using decorrelated discriminators. The search is performed using events with 0, 1, or 2 electrons or muons in conjunction with at least six jets. No requirement is placed on the magnitude of the missing transverse momentum. The result is based on a sample of proton-proton collisions at $\sqrt{s} = 13\,\text{TeV}$ corresponding to $138\,\text{fb}^{-1}$ of integrated luminosity collected with the CMS detector at the LHC in 2016–2018. With no statistically significant excess of events observed beyond the expected contributions from the standard model, the data are used to determine upper limits on the top squark pair production cross section in the frameworks of RPV and stealth SUSY. Models with top squark masses less than 700 (930) GeV are excluded at 95% confidence level for RPV (stealth) SUSY scenarios.

Published in the Journal of High Energy Physics as doi:10.1007/JHEP10(2025)236.

*See Appendix B for the list of collaboration members

1 Introduction

The standard model (SM) of particle physics describes observed phenomena of elementary particles with incredible precision. Despite this success, there remain many questions unanswered by the SM that inspire a continuing search for new particles and phenomena predicted by theories beyond the SM (BSM). Supersymmetry (SUSY) is a long-sought-after BSM framework that addresses several shortcomings of the SM including the gauge hierarchy problem, in which radiative corrections to the Higgs boson mass parameter, especially those associated with the top quark, are quadratically divergent. In SUSY, this hierarchy problem can be mitigated by the presence of a light bosonic top squark $\widetilde{\mathrm{t}}$, which, as the supersymmetric partner of the top quark, brings an additional set of radiative corrections that largely cancel the divergent SM corrections [1, 2]. Historically, searches for strong production of $\widetilde{\mathrm{t}}$ squarks have focused on final states with large missing transverse momentum $p_{\mathrm{T}}^{\text{miss}}$ related to the undetected lightest SUSY particle (LSP) produced in $\widetilde{\mathrm{t}}$ squark decays; strong limits have been placed on $\widetilde{\mathrm{t}}$ squark production in this context [3–10]. However, well-motivated variants of SUSY can produce final states without large $p_{\mathrm{T}}^{\text{miss}}$ including SUSY with R-parity violation (RPV) [11, 12] and "stealth" SUSY [13–15].

In this analysis, we search for $\widetilde{\mathrm{t}}$ squark pair production with decays in both the RPV and stealth SUSY frameworks. In RPV SUSY, additional superpotential terms allow the LSP to decay into SM particles, thereby producing a signature with balanced transverse momentum p_{T}. The RPV coupling governing hadronic decays of SUSY particles is denoted by λ''_{abc} where a, b, c indicate the generation of the one up-type and two down-type quarks involved in the decay vertex [11]. In the benchmark RPV model considered here, each $\widetilde{\mathrm{t}}$ squark decays to a top quark t and a neutralino $\widetilde{\chi}_1^0$, followed by the RPV decay of the $\widetilde{\chi}_1^0$ to three light-flavor quarks, $\widetilde{\chi}_1^0 \to \mathrm{qqq}$. Since the analysis is insensitive to differences between jets originating from quarks of the first and second generations, the results are applicable to RPV models with coupling λ''_{abc} where $a, b, c \in \{1, 2\}$. The stealth SUSY $\mathrm{SY\overline{Y}}$ model [14] assumes a new hidden sector containing a scalar particle S with even R-parity and its superpartner $\widetilde{\mathrm{S}}$, both of which are singlets under all SM interactions [13]. The key feature of stealth SUSY is that supersymmetry is approximately conserved in the hidden sector, resulting in nearly mass-degenerate $\widetilde{\mathrm{S}}$ and S without artificial tuning of particle masses. In the benchmark $\mathrm{SY\overline{Y}}$ model, each $\widetilde{\mathrm{t}}$ squark decays to a top quark, gluon g, and a singlino $\widetilde{\mathrm{S}}$, with the $\widetilde{\mathrm{S}}$ decay contributing a gravitino $\widetilde{\mathrm{G}}$ and two additional gluons to the final state, as shown in Fig. 1. Because of the small S–$\widetilde{\mathrm{S}}$ mass difference and small $\widetilde{\mathrm{G}}$ mass, the undetected $\widetilde{\mathrm{G}}$ results in negligible observed $p_{\mathrm{T}}^{\text{miss}}$.

The CMS Collaboration at the CERN LHC published a search for these signals in 2021 [16] based on the full Run 2 data set that considered final states with exactly one lepton and at least seven jets. The results showed a maximum local signal significance of 2.8 standard deviations for a $\widetilde{\mathrm{t}}$ squark mass $m_{\widetilde{\mathrm{t}}}$ of 400 GeV in the RPV model, arising primarily from terms in the fit likelihood for constrained nuisance parameters associated with the systematic uncertainty in the shape of the jet multiplicity (N_{jets}) distribution for the dominant $\mathrm{t\bar{t}}$ + jets background.

The search presented in this paper extends and improves on the previous analysis in two ways.

First, to better evaluate whether any observed discrepancy arises in events with two top quarks in the final state, we now consider all three $\mathrm{t\bar{t}}$ decay channels: all-hadronic (0ℓ), single-lepton (1ℓ), and fully leptonic (2ℓ). This results in a $\approx$30% improvement in the expected upper limit on the $\widetilde{\mathrm{t}}$ squark pair production cross section for the RPV signal model with $m_{\widetilde{\mathrm{t}}} = 850$ GeV (near the previous exclusion limit on $m_{\widetilde{\mathrm{t}}}$).

Second, the method for estimating the primary $\mathrm{t\bar{t}}$ + jets background from data has been up-

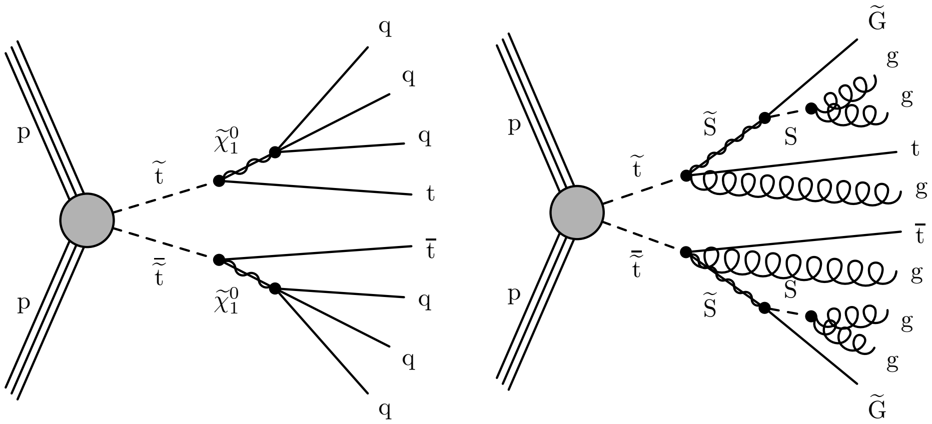

Figure 1: Diagrams of top squark pair production with each squark decaying to a top quark and additional light-flavor quarks for the RPV SUSY model (left) and with each squark decaying to a top quark, gluons, and a gravitino for the stealth SY$\overline{\text{Y}}$ model (right).

dated to reduce the dependence of the analysis on systematic uncertainties related to the N_{jets} modeling in $\text{t}\overline{\text{t}}$ + jets events [16]. In the previous analysis, the maximum likelihood fit, which provides a simultaneous estimate of the $\text{t}\overline{\text{t}}$ + jets background and signal, relied on modeling of the shape of the N_{jets} distribution for the background. In the current analysis, however, the fit employs independent background yield parameters for each N_{jets} category. These yield parameters are constrained using an effective sideband extrapolation in two independent neural network (NN) variables that discriminate signal from the background (called $S_{\text{NN,1}}$ and $S_{\text{NN,2}}$), which are generated according to the ABCDisCo Training Enhanced with Closure (ABCDisCoTEC) method [17]. This method augments the ABCDisCo technique [18], which minimizes the distance correlation between $S_{\text{NN,1}}$ and $S_{\text{NN,2}}$, by also directly minimizing the nonclosure of the sideband extrapolation in the NN training. This technique yields an overall reduction in systematic uncertainty arising from possible discrepancies in the shape of the N_{jets} spectrum. The expected upper limit on the $\widetilde{\text{t}}$ squark pair production cross section has improved by a factor of ≈2 at low $m_{\widetilde{\text{t}}}$ (between 300 and 450 GeV) for both signal models as a result of this improvement.

The detector and general experimental techniques are described in Section 2, followed by a discussion of the simulated samples in Section 3. The event selection is detailed in Section 4. Section 5 outlines the ABCDisCoTEC method and its application in this analysis. The background estimation and treatment of systematic uncertainties are detailed in Section 6 and 7, respectively. Finally, the results and their interpretation are described in Section 8, followed by a summary in Section 9. Tabulated results are provided in the HEPData record for this analysis [19].

2 Experimental techniques

This search examines proton-proton (pp) collision data at $\sqrt{s} = 13$ TeV collected during 2016–2018 with the CMS detector at the LHC corresponding to an integrated luminosity of 138 fb^{-1} [20–22]. The CMS apparatus [23, 24] is a multipurpose, nearly hermetic detector, designed to trigger on [25–27] and identify electrons, muons, photons, and (charged and neutral) hadrons [28–30]. Its central feature is a superconducting solenoid of 6 m internal diameter, providing a magnetic field of 3.8 T. Within the solenoid volume are a silicon pixel and strip tracker, a lead tungstate crystal electromagnetic calorimeter (ECAL), and a brass and scintillator hadron calorimeter (HCAL), each composed of a barrel and two endcap sections. Forward calorimeters extend the pseudorapidity coverage provided by the barrel and endcap detectors. Muons are reconstructed in gas-ionization detectors embedded in the steel flux-return yoke outside the solenoid. More detailed descriptions of the CMS detector, together with a definition of the coordinate system used and the relevant kinematic variables, can be found in Refs. [23, 24].

The primary vertex (PV) is taken to be the vertex corresponding to the hardest scattering in the event, evaluated using tracking information alone, as described in Section 9.4.1 of Ref. [31]. A particle-flow algorithm [32] aims to reconstruct and identify each individual particle in an event, with an optimized combination of information from the various elements of the CMS detector. The energy of photons is obtained from the ECAL measurement. The energy of electrons is determined from a combination of the electron momentum at the PV as determined by the tracker, the energy of the corresponding ECAL cluster, and the energy sum of all bremsstrahlung photons spatially compatible with originating from the electron track. The energy of muons is obtained from the curvature of the corresponding track. The energy of charged hadrons is determined from a combination of their momentum measured in the tracker and the matching ECAL and HCAL energy deposits, corrected for the response function of the calorimeters to hadronic showers. Finally, the energy of neutral hadrons is obtained from the corresponding corrected ECAL and HCAL energies.

For each event, hadronic jets are clustered from these reconstructed particles using the anti-k_T algorithm [33, 34] with a distance parameter of 0.4. Jet momentum is determined as the vectorial sum of all particle momenta in the jet, and is found from simulation to be, on average, within 5 to 10% of the true momentum over the whole p_T spectrum and detector acceptance. Additional pp interactions within the same or nearby bunch crossings (pileup) can contribute additional tracks and calorimetric energy depositions to the jet momentum. To mitigate this effect, charged particles identified to be originating from pileup vertices are discarded and an offset correction is applied to correct for remaining contributions [35]. Jet energy corrections are derived from simulation studies so that the average measured energy of jets becomes identical to that of particle level jets. In situ measurements of the momentum balance in dijet, photon + jet, Z + jet, and multijet events are used to determine any residual differences between the jet energy scale in data and in simulation, and appropriate corrections are made [36]. Additional selection criteria are applied to each jet to remove jets potentially dominated by instrumental effects or reconstruction failures [35].

For this analysis, reconstructed jets are required to have $p_T > 30\,\text{GeV}$ and $|\eta| < 2.4$. Jets that overlap with a lepton meeting the analysis requirements within a cone of radius $\Delta R = \sqrt{(\Delta\phi)^2 + (\Delta\eta)^2} = 0.4$ are removed. These jets are evaluated using the "medium" working point of the DeepJet tagging algorithm designed to identify jets as arising from bottom quark fragmentation (b-tagged jet). For jets with $p_T \approx 30\,\text{GeV}$, the efficiency of the algorithm is $\approx$75% with a misidentification rate for light-flavor jets and gluon jets of 1% [37–39].

Electrons are required to pass a "tight" level of identification that is around 70% efficient in electron identification [28, 40]. All electrons in this analysis are required to meet the requirements of $p_T > 30\,\text{GeV}$ and $|\eta| < 2.4$. For data in 2017–2018, the p_T threshold is raised to 37 GeV to accommodate higher trigger thresholds. The transverse and longitudinal impact parameters of the electron track from the PV are required to be less than 0.05 (0.10) cm in the barrel (endcap) and less than 0.10 (0.20) cm in the barrel (endcap), respectively.

Muons are required to pass a "medium" level of identification that is around 98% efficient for genuine muon identification [29]. Muons are additionally required to have $p_T > 30\,\text{GeV}$ and

$|\eta| < 2.4$. The transverse (longitudinal) impact parameters of the muon track from the PV are required to be less than 0.2 (0.5) cm, respectively.

Additionally, electrons and muons are required to be isolated from nearby detector activity, as defined by the requirement that the ratio of the p_{T} sum of other objects in a cone surrounding the lepton to the p_{T} of the lepton itself be less than 0.1 (0.2) for electrons (muons), where the radius of the cone scales as $1/p_{\mathrm{T}}$ [41] and ranges from a minimum of 0.05 for leptons with $p_{\mathrm{T}} > 200\,\mathrm{GeV}$ to a maximum of 0.2 for $p_{\mathrm{T}} < 50\,\mathrm{GeV}$.

In addition to the muons defined above, a second collection of muons is used to define a control region (CR) for multijet production from quantum chromodynamics (QCD multijet). These muons, called nonisolated muons, have the same "medium" identification, η, and impact parameter requirements as standard muons, but they are required to have $p_{\mathrm{T}} > 55\,\mathrm{GeV}$ and the isolation requirement is reversed.

Events of interest are selected using a two-tiered trigger system. The first level (L1), composed of custom hardware processors, uses information from the calorimeters and muon detectors to select events at a rate of around 100 kHz within a fixed latency of $4\,\mu$s [25]. The second level, known as the high-level trigger, consists of a farm of processors running a version of the full event reconstruction software optimized for fast processing, and reduces the event rate to around 1 kHz before data storage [26].

For the 0ℓ channel, a collection of triggers that target large amounts of hadronic activity and b-tagged jets are employed. The most efficient of these triggers requires six jets with $p_{\mathrm{T}} > 40\,\mathrm{GeV}$, a b-tagged jet, and the scalar p_{T} sum of all jets, H_{T}, to be above 450 (430) GeV, for data collected in 2016 (2017–2018). Additional hadronic triggers are also included that require events to have at least one jet with $p_{\mathrm{T}} > 450\,(500)\,\mathrm{GeV}$ or $H_{\mathrm{T}} > 900\,(1050)\,\mathrm{GeV}$, with no other restrictions, for data collected in 2016 (2017–2018). In 2016, this combination of triggers achieves an overall efficiency of 85–90% near the thresholds of $H_{\mathrm{T}} > 450\,\mathrm{GeV}$ or $p_{\mathrm{T}} > 40\,\mathrm{GeV}$ for the sixth highest ranked p_{T} jet. In 2017–2018, among events with only one b-tagged jet (at least 2 b-tagged jets), the overall efficiency is about 55 (80)% near the thresholds of $H_{\mathrm{T}} > 500\,\mathrm{GeV}$ or sixth jet $p_{\mathrm{T}} > 40\,\mathrm{GeV}$.

In both the 1ℓ and 2ℓ channels, events are selected with triggers requiring at least one electron or one muon. The lowest p_{T} thresholds for these triggers in 2016 (2017–2018) are 27 (35) GeV for electrons and 24 (24) GeV for muons. Additionally, the leptons are required to be isolated from tracks and from calorimeter activity. Lepton triggers without isolation requirements are also used with higher thresholds of 115 GeV for electrons and 50 GeV for muons. All leptonic triggers are combined for an overall efficiency ranging from about 70% for leptons with p_{T} near the trigger threshold to above 85% for $p_{\mathrm{T}} > 120\,\mathrm{GeV}$. The single-muon trigger with the 50 GeV p_{T} threshold is additionally used to populate the QCD multijet CR. The efficiency of this trigger alone is about 90% for muons with $p_{\mathrm{T}} > 100\,\mathrm{GeV}$.

During the 2016 and 2017 data taking, a gradual shift in the timing of the inputs of the ECAL L1 trigger in the region at $|\eta| > 2.0$ caused a specific trigger inefficiency. For events containing an electron (a jet) with p_{T} larger than $\approx$50 GeV ($\approx$100 GeV), in the region $2.5 < |\eta| < 3.0$, the efficiency loss is $\approx$10–20%, depending on p_{T}, η, and time.

3 Simulated samples

Simulated samples are used to estimate contributions from minor backgrounds to the search region (SR) yields, to model the signal contribution in the SR, to estimate systematic uncertainties, and to serve as inputs (signal and $\mathrm{t\bar{t}}$) to the training of NNs.

Top quark pair production, t-channel single top quark production, and single top quarks produced in association with a W boson are generated with the next-to-leading order (NLO) POWHEG v2.0 generator [42–47]. The MADGRAPH5_aMC@NLO v2.6.5 generator [48] is used in NLO mode for $\mathrm{t\bar{t}} + \mathrm{W/Z/H}$, $\mathrm{t\bar{t}t\bar{t}}$, tZq, and s-channel single top quark production events, while leading order (LO) mode is used for QCD multijet, $\mathrm{t\bar{t}}$ + diboson/tW/t + jet, Drell–Yan, and W + jets production. Diboson production is generated at LO with PYTHIA v8.240 [49]. Samples are normalized to production cross sections calculated to the highest available accuracy, generally NLO or next-to-NLO (NNLO) [48, 50–56].

For the signal, top squarks are produced with MADGRAPH5_aMC@NLO in LO mode with up to two additional partons at the matrix element level and their decays are simulated with PYTHIA. Signal production cross sections ($\sigma_{\widetilde{\mathrm{t}}\bar{\widetilde{\mathrm{t}}}}$) are approximated to NNLO plus next-to-next-to-leading logarithmic (NNLL) accuracy [57–61]. A range of $m_{\widetilde{\mathrm{t}}}$ is considered from 300 to 1050 GeV, and all decays are assumed to be prompt with branching fractions of unity. In the benchmark RPV model, we take the $\widetilde{\chi}^0_1$ mass to be 100 GeV, which ensures an on-shell top quark in the $\widetilde{\mathrm{t}}$ squark decay for all $m_{\widetilde{\mathrm{t}}}$. For the benchmark stealth SY$\overline{\mathrm{Y}}$ model, the characteristic small S–$\widetilde{\mathrm{S}}$ mass difference is held constant at 10 GeV, and we assume an $\widetilde{\mathrm{S}}$ mass of 100 GeV and a $\widetilde{\mathrm{G}}$ mass of 1 GeV.

Hadronization and parton showering is done by PYTHIA using underlying event (UE) tune CP5 [62, 63]. Parton distribution functions (PDFs) from the NNPDF3.1 NNLO set [64] are used for all processes. The CMS detector response is modeled in simulation using GEANT4 [65]. This response is then passed through the same event reconstruction as collision data.

In order to match the instantaneous luminosity profile measured at the CMS detector, simulated events are reweighted based on the distributions of the observed and simulated number of pp interactions per bunch crossing. Corrections related to the efficiencies of the trigger system (including for the ECAL timing shift), lepton identification and isolation (for the 1ℓ and 2ℓ channels), b tagging, and top quark tagging (for the 0ℓ channel) are applied to simulated events in order to mitigate small differences observed with respect to data. These corrections are calculated by comparing the efficiency of object identification in simulation to that in data.

4 Event selection

The dominant background for the search arises from top quark pair production with additional jets from initial- and final-state radiation (ISR and FSR). The primary physical observable that allows discrimination of signal from $\mathrm{t\bar{t}}$ + jets background is N_{jets}, which is enhanced in the signal. QCD multijet production is the subdominant background with additional minor backgrounds from production of $\mathrm{t\bar{t}}$ in association with SM weak gauge bosons or additional top quarks ($\mathrm{t\bar{t}}$+X), production of weak gauge bosons, and single top quark production—all with additional jets from ISR or FSR. The QCD multijet and other non-$\mathrm{t\bar{t}}$ backgrounds are suppressed via selection criteria related to the presence of a top quark. We require either one or two charged leptons (e or μ) or, for events with zero charged leptons, the identification of a top quark via a top quark tagging algorithm. Further suppression is obtained with requirements based on the presence of b-tagged jets.

The selection criteria for the three search channels are summarized in Table 1. The three search region selections are defined orthogonally using exact selections on the number of isolated leptons $N^{\text{iso}}_{\text{leptons}}$. Each selection is defined such that it is more restrictive than the trigger re-

Table 1: Search region selections for the 0ℓ, 1ℓ, and 2ℓ channels. The term $N_{\text{muon}}^{\text{noniso}}$ denotes the number of nonisolated muons.

Selection criteria	0ℓ	1ℓ	2ℓ
$N_{\text{leptons}}^{\text{iso}}$	0	1	2, oppositely charged
$N_{\text{muon}}^{\text{noniso}}$	0	0	0
H_T (GeV)	>500	>500	>500
N_{jets} $(p_T > 30\,\text{GeV})$	≥8	≥7	≥6
N_{jets} $(p_T > 45\,\text{GeV})$	≥6	—	—
N_b $(p_T > 30\,\text{GeV})$	≥2	≥1	≥1
N_b $(p_T > 45\,\text{GeV})$	≥1	—	—
N_t	≥2	—	—
$M_{b\ell}$ (GeV)	—	>50, <250	—
$M_{\ell\ell}$ (GeV)	—	—	<81 or >101
ΔR_{bjets}	>1	—	—

quirements for jets, leptons, and H_T for the respective channels. The particular N_{jets} selection for each channel follows from the leptonic versus hadronic decay of each W boson, while also considering effects from detector acceptance and contributions from other backgrounds. Additional restrictions are placed on the jets for the 0ℓ channel to match the jet p_T requirements in the trigger. Jets passing these additional restrictions are a subset of the jets that pass the less strict p_T requirement.

Each of the three search channels is also defined with dedicated selections to enhance background rejection based on the unique final-state topology of each channel. The 0ℓ channel selection requires at least two b-tagged jets (N_b), which are angularly separated by $\Delta R_{\text{bjets}} > 1$ to minimize the QCD multijet event yield. This background is further reduced by requiring at least two tagged top quark objects (N_t) identified by an NN-based hadronic top quark tagging algorithm [6, 66]. The t tagging algorithm employs two different NNs, with one network trained to identify low-p_T top quarks ($\lesssim$400 GeV) that decay to three individually resolved jets, and the other to identify high-p_T top quarks from single jets clustered with the anti-k_T algorithm with a distance parameter of 0.8. The working point for the t tagging algorithm is optimized in order to maximize statistical significance in the 0ℓ search channel. The average efficiency for the two taggers is ≈40%.

The 1ℓ channel event selection imposes that the invariant mass of the required b-tagged jet and lepton ($M_{b\ell}$) be between 50 and 250 GeV to loosely tag the leptonically decaying top quark in the event. Finally, the 2ℓ selection requires that the invariant mass of the two oppositely charged leptons ($M_{\ell\ell}$) be distant from the Z boson mass resonance peak in order to reduce the Drell–Yan background.

For each of the three analysis channels, a unique QCD multijet CR is used to estimate the QCD multijet event yield in the SR. These events are identified by the presence of a nonisolated muon along with the same requirements for N_{jets} and H_T used for the corresponding SR definitions. The requirement of exactly one nonisolated muon ensures that the CR is sufficiently pure in multijet events and matches the trigger requirements. No additional requirements are placed on N_b or N_t.

Simulated background events passing the SR selection requirements for a given analysis channel predominantly originate from $t\bar{t}$ + jets production, with contributions of less than 7% from QCD multijet processes, and a few percent from the remaining minor backgrounds.

5 The ABCDisCoTEC method

The ABCD method [67, 68] is a common background estimation technique that uses data CRs to extrapolate the background into the signal region. The method's success depends on choosing two quantities that are independent from each other and can distinguish between signal and background. Having chosen two independent quantities, four regions are constructed in a two-dimensional (2D) plane with each quantity defining an axis of the plane. These regions are created by imposing selection criteria on both quantities. The CRs are subsequently referred to as B, C, D and cover the domain of the plane that is mostly populated by background events. B and C contain events which pass only one of the selection criteria while D contains events passing neither. The region subsequently referred to as A is the remaining portion of the plane where signal events are predominantly expected to reside. All events contained in A pass the selection criteria imposed on both quantities. Assuming independence of the two quantities defining this 2D ABCD plane, the number of background events in the SR A can be predicted by using the B, C, D CRs via the relationship

$$N_{A,\,\text{pred.}} = (N_B N_C)/N_D, \tag{1}$$

where N_i (with $i = B, C, D$) is the number of events in CR i, and $N_{A,\,\text{pred.}}$ is the number of predicted background events in the SR A.

In practice, it is not always straightforward to identify two statistically independent quantities that also provide sufficient signal sensitivity. If the final states of signal and background events are naturally similar to one another (as is the case for the signal models considered in this analysis), then simple object- or event-level quantities may not be sufficient to perform the ABCD method and be sensitive to signal. Rather than relying on physical quantities for defining the ABCD plane, one can generate two synthetic quantities satisfying the ABCD criterion above using the so-called Double Disco NN [18], which includes a statistical measure of nonlinear dependence known as distance correlation (DisCo) [69] in the loss function to impose independence of its two simultaneously trained binary classifiers. The ABCDisCoTEC method used in this paper augments the Double DisCo NN with additional features including a novel loss term that directly minimizes the nonclosure of the ABCD method using a metric proportional to $(N_A N_D - N_B N_C)^2$, where N_A is the number of events in the SR A. A more detailed description of the ABCDisCoTEC NN model can be found in Ref. [17].

6 Background estimation

6.1 Implementing the ABCDisCoTEC method for the $t\bar{t}$ background

For this search, the ABCDisCoTEC NN model is specifically trained to discriminate between the main $t\bar{t}$ + jets background and RPV or stealth $SY\overline{Y}$ signal models. A separate training of the model is performed for each of the three lepton channels and each of the signal models, resulting in a total of six independent NN trainings. For each training, a mixture of simulated signal events with $m_{\tilde{t}}$ ranging from 300 to 1400 GeV in 50 GeV increments is used. To make the trained NNs more robust to potential differences between simulation and data, the training samples include not only events from the nominal simulation, but also events simulated with systematic variations in the physics modeling and event reconstruction. Simulated $t\bar{t}$ + jets events include variations in the matching scale between the matrix element and parton shower (ME-PS) [70], the UE tune [62], and the modeling of color reconnection in the parton shower in PYTHIA [63], all of which have an impact on N_{jets}. Variations in jet energy resolution (JER) and scale (JES) are included for both simulated $\text{t}\bar{\text{t}} + \text{jets}$ and signal events. Both up- and down-type variations (i.e. ± 1 standard deviation for each systematic uncertainty) are included in the training set. Finally, to test the NN model's performance and generalization, 80% of the available simulated events are used for training, while the remaining 20% are reserved for validation.

All NN input variables are computed in an approximate center-of-mass frame defined by all jets in the event with $p_{\text{T}} > 30\,\text{GeV}$ and $|\eta| < 5$. Properties for the first six (2ℓ channel), seven (1ℓ channel), or eight (0ℓ channel) jets, including their four-vectors and flavor tagging information, are used. Likewise, for the 1ℓ and 2ℓ channels, the four-vector(s) of the lepton(s) are used as inputs. In addition to these low-level quantities, higher-level quantities are input to the NN, including Fox–Wolfram moments [71], the eigenvalues of the jet energy-momentum tensor [72], and the two four-vectors of reconstructed event "hemispheres," which are constructed through the object clustering method described in Refs. [73, 74]. For background (signal), each clustered hemisphere typically contains the decay products of one of the two top quarks (squarks) in the event.

As mentioned previously, N_{jets} is the main feature distinguishing signal from background, and sensitivity to signal is maximized at high N_{jets}. To ensure that the training of the NN model is not dominated by the large number of low-N_{jets} events in the simulation, all N_{jets} categories are equally sampled during the NN training.

Figure 2 shows the distributions of $S_{\text{NN},1}$ and $S_{\text{NN},2}$, integrated over all N_{jets} categories, for the training for the 1ℓ channel and the RPV signal model for both data and simulation. Note that as the $\text{t}\bar{\text{t}} + \text{jets}$ estimate ultimately used in the analysis comes from the fit to data, the level of agreement between data and pre-fit simulation in the upper figures does not impact the background prediction. The 2D probability density functions for $\text{t}\bar{\text{t}} + \text{jets}$ and signal simulations are smoothed with Gaussian kernel density estimation.

6.2 The ABCD region definition and correction factor derivation

The optimal values of $S_{\text{NN},1}$ and $S_{\text{NN},2}$ for dividing the $S_{\text{NN},1}$-$S_{\text{NN},2}$ plane into A, B, C, D regions (ABCD bin boundaries) are determined with a grid search over $S_{\text{NN},1}$ and $S_{\text{NN},2}$ considering four figures of merit (FOMs): the expected signal significance and the upper limit on the signal cross section for signal models with $m_{\tilde{\text{t}}}$ of 400 and 800 GeV. For each point in the scans, the complete simultaneous fit with full treatment of systematic uncertainties is performed in simulation. For each lepton channel and signal model, we use two bin boundary choices optimized separately for low and high $m_{\tilde{\text{t}}}$ in order to improve the performance across the full considered $m_{\tilde{\text{t}}}$ range; the low-mass boundary is used for RPV (stealth $\text{SY}\overline{\text{Y}}$) signals with masses less than 625 (675) GeV. The FOM used for determining the optimal low- (high-)mass boundaries is the signal significance (cross section limit) for the model with $m_{\tilde{\text{t}}}$ of 400 (800) GeV. The significance is chosen as the FOM for low $m_{\tilde{\text{t}}}$ to target the region in which the previous analysis observed an excess for the RPV model with $m_{\tilde{\text{t}}} = 400\,\text{GeV}$ described in Section 1. Finally, for each lepton channel and signal model, the same bin boundary is used for all N_{jets} categories. A summary of the optimal bin boundaries is shown in Table 2.

To account for residual correlation between $S_{\text{NN},1}$ and $S_{\text{NN},2}$, a correction factor κ is obtained from $\text{t}\bar{\text{t}} + \text{jets}$ simulation and is applied to the $\text{t}\bar{\text{t}} + \text{jets}$ prediction in the maximum likelihood fits. A separate κ factor is calculated from the ratio of observed and predicted A region events

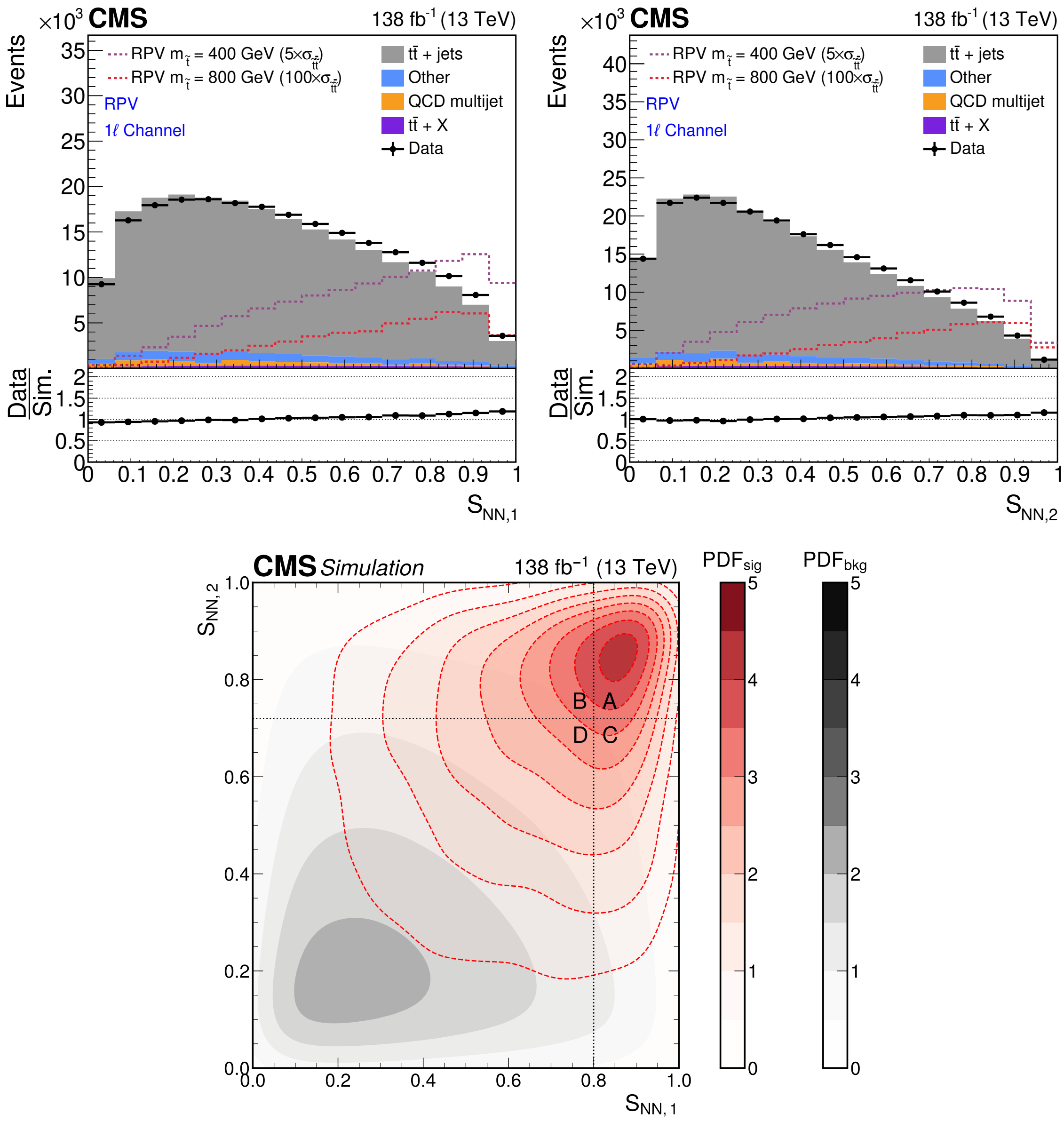

Figure 2: For the RPV signal model and all N_{jets} categories of the 1ℓ channel, distributions of $S_{\text{NN},1}$ (upper left) and $S_{\text{NN},2}$ (upper right) for data (black solid line), pre-fit simulated SM backgrounds (stacked filled histograms), and two RPV signal models with $m_{\tilde{t}} = 400$ and $800\,\text{GeV}$ (dashed lines) are shown. The lower panel shows the two-dimensional probability density function distribution of $S_{\text{NN},1}$ and $S_{\text{NN},2}$ for simulated $\text{t}\bar{\text{t}} + \text{jets}$ events (solid gray) and the RPV signal model with $m_{\tilde{t}} = 800\,\text{GeV}$ (dashed red). The ABCD bin boundaries for this signal model in the 1ℓ channel are shown with dashed vertical and horizontal lines.

Table 2: Values of $(S_{\mathrm{NN},1}, S_{\mathrm{NN},2})$ defining the ABCD bin boundaries for the low- and high-mass optimizations for each lepton channel and signal model.

Signal model	Lepton channel	Low-mass boundaries	High-mass boundaries
RPV	0ℓ	(0.52, 0.54)	(0.74, 0.80)
RPV	1ℓ	(0.84, 0.42)	(0.80, 0.72)
RPV	2ℓ	(0.52, 0.58)	(0.50, 0.50)
$\mathrm{SY\overline{Y}}$	0ℓ	(0.76, 0.70)	(0.54, 0.56)
$\mathrm{SY\overline{Y}}$	1ℓ	(0.44, 0.42)	(0.68, 0.82)
$\mathrm{SY\overline{Y}}$	2ℓ	(0.40, 0.42)	(0.48, 0.48)

for each N_{jets} category, signal model, lepton channel, and low- or high-mass range:

$$\kappa = \frac{N_{A,\,\mathrm{MC}}}{N_{A,\,\mathrm{pred.}}} = \frac{N_{A,\,\mathrm{MC}}\,N_{D,\,\mathrm{MC}}}{N_{B,\,\mathrm{MC}}\,N_{C,\,\mathrm{MC}}}, \tag{2}$$

where $N_{A,\,\mathrm{pred.}}$ is obtained from Eq. (1). For a perfect ABCDisCoTEC training, each κ would be equal to one. Values for all sixty κ factors range from 0.875 to 1.887 with statistical uncertainties ranging from 0.008 to 0.12.

6.3 Maximum likelihood fit

A set of simultaneous binned maximum-likelihood fits (over the range of $m_{\tilde{t}}$) is performed for each signal model and lepton channel for a total of six sets of fits. In addition, a combined fit over all three lepton channels is performed for each signal model. Each fit estimates the signal and background yields in twenty analysis regions comprising the four A, B, C, D regions in each of five N_{jets} categories. The number of jets in the N_{jets} categories for each lepton channel range from 8 to $\geq$12 jets for the 0ℓ channel, 7 to $\geq$11 jets for the 1ℓ channel, and 6 to $\geq$10 jets for the 2ℓ channel. In each fit, the $\mathrm{t\bar{t}}+$jets background yields for the twenty analysis regions are included as floating parameters b_i^j with j denoting N_{jets} category and i denoting ABCD region. The four b_i^j yields in each N_{jets} category are subject to the ABCD constraint from Eq. (1) including the correction factor κ^j from Eq. (2) as

$$b_A^j = \kappa^j (b_B^j b_C^j)/b_D^j. \tag{3}$$

Each fit includes a single free parameter determining the overall signal normalization (referred to as the signal strength) with the distribution of signal events across the twenty analysis regions fixed according to simulation. In addition to the b_i^j parameters and the signal strength, each fit includes constrained nuisance parameters which are allowed to vary, accounting for a range of systematic uncertainties.

For each fit, the QCD multijet background in each of the twenty analysis regions is fixed according to an estimate from the corresponding signal-depleted QCD multijet data CR and using the corresponding ABCD bin boundaries for each channel, signal, and mass optimization. A transfer factor relating the number of simulated QCD multijet events in the SRs and CRs is used to scale the QCD multijet component of data in the CR for use as the analysis region prediction. This transfer factor ranges from 0.0002 to 0.4 over all analysis regions and fits. The remaining minor backgrounds are fixed according to the simulation.

7 Systematic uncertainties

The key assumption governing the $t\bar{t}$ + jets background estimation is that the ABCD relationship holds. By definition, the correction factor κ defined in Eq. (2) ensures that this is the case in simulation. We evaluate the residual nonclosure of the ABCD relationship in data (after application of the κ correction) and determine a related systematic uncertainty with a two-fold process performed separately for each lepton channel (0ℓ, 1ℓ, 2ℓ), signal model (RPV or stealth $SY\overline{Y}$), and ABCD boundary choice (low- or high-mass).

First, we use three signal-depleted data validation regions (VRs) in which the ABCD relationship should hold to evaluate a residual nonclosure metric $\mathcal{C}$, defined as

$$\mathcal{C} = 1 - \frac{\kappa N_{A,\,\text{pred.}}}{N_A} = 1 - \frac{\kappa N_B N_C}{N_A N_D}. \tag{4}$$

As illustrated in Fig. 3, the region VR I (VR II) is defined as approximately the combination of the nominal BD (CD) region, and thus spans the full $S_{\text{NN},2}$ ($S_{\text{NN},1}$) range. The ABCD subregions of VR I (VR II) are defined by bisecting VR I (VR II) on the $S_{\text{NN},1}$ ($S_{\text{NN},2}$) axis while keeping the nominal boundary on $S_{\text{NN},2}$ ($S_{\text{NN},1}$) constant. The region VR III comprises the D region and is bisected on both S_{NN} axes to create the ABCD subregions. In order to address potential dependence of $\mathcal{C}$ on the location of the ABCD bin boundaries, the boundaries of each VR (and its ABCD subregions) are moved in steps towards the nominal ABCD bin boundaries and $\mathcal{C}$ is calculated at each step as described in Ref. [17]. The N_i counts used in each calculation are taken from the data after subtraction of non-$t\bar{t}$ background according to simulation. Only those ABCD subregions with an expected signal fraction less than 5% are considered in the nonclosure study. The systematic uncertainty associated with the residual nonclosure in data (data-based nonclosure systematic uncertainty) for a given search channel, signal model, and ABCD bin boundary is taken as the largest deviation of $\mathcal{C}$ from unity from all three VR scans for the lowest N_{jets} category. Categories at higher N_{jets} do not have a sufficient number of steps in the procedure passing the 5% signal fraction requirement to provide an uncertainty estimate. Therefore, the same uncertainty is used for all N_{jets} categories. Values of this uncertainty range from 3 to 15%.

Second, to account for potential additional effects on the residual nonclosure in data at high N_{jets}, we use simulated $t\bar{t}$ + jets samples in which various aspects of $t\bar{t}$ + jets modeling are varied including ISR and FSR, ME-PS matching, UE tune, color reconnection, JES, and JER. The same process for calculating κ is applied to these varied $t\bar{t}$ + jets samples and any difference in κ between the nominal and varied samples is taken as a systematic uncertainty for cases in which the change in κ exceeds the statistical uncertainty summed in quadrature with the residual nonclosure systematic uncertainty described above; the only modeling variation for which κ meets this requirement is that related to FSR. This uncertainty has a typical size of 10–20% on the $t\bar{t}$ + jets normalization, but can be as large as 96% for the highest N_{jets} category in the 0ℓ region. The statistical uncertainty in the nominal κ factor is also included as a systematic uncertainty in the $t\bar{t}$ + jets prediction.

Figure 4 shows the maximum $\mathcal{C}$ in data for each N_{jets} category across the VRs and ABCD bin boundaries with expected signal fraction less than 5% for the RPV low-mass optimization. For N_{jets} categories in which no VR and ABCD bin boundaries satisfy this requirement, the statistical uncertainty in $\mathcal{C}$ for the boundaries listed in Table 2 is shown. Also shown are the deviations from one of the simulation-based closure correction κ, the FSR systematic uncertainty, and the total statistical and systematic uncertainty for the $t\bar{t}$ + jets prediction. In all cases, $\mathcal{C}$ is comparable to the total systematic uncertainty. In addition, we observe that $\mathcal{C}$ is small even if κ is larger

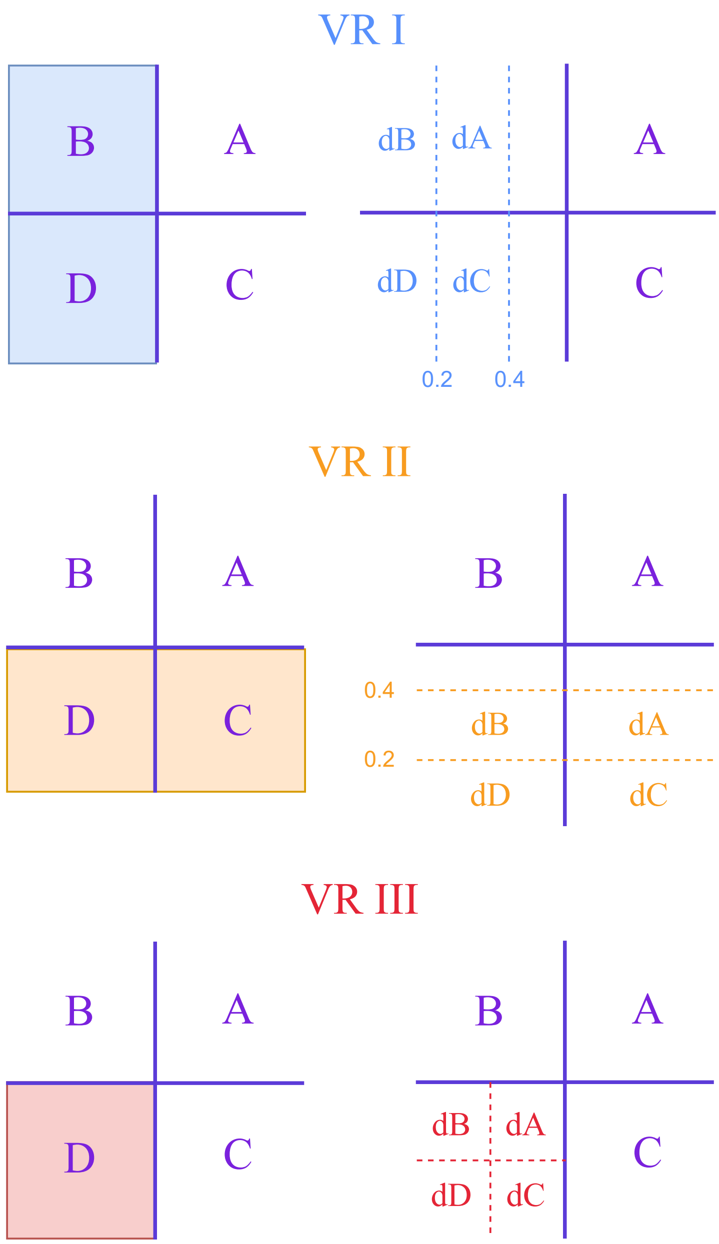

Figure 3: Illustrations of the three validation regions that are created by partitioning the $S_{NN,1}$-$S_{NN,2}$ plane. VR I (VR II), shown in the upper (middle) row, is a division of the B and D (C and D) regions. VR III (lower row) is a division of the D region. Each VR is divided into four subregions (dA, dB, dC, dD) that are used to perform the validation of the nonclosure of the $S_{NN,1}$-$S_{NN,2}$ plane. The subregion boundaries shown in the figure are the starting points of the stepping procedure explained in the text.

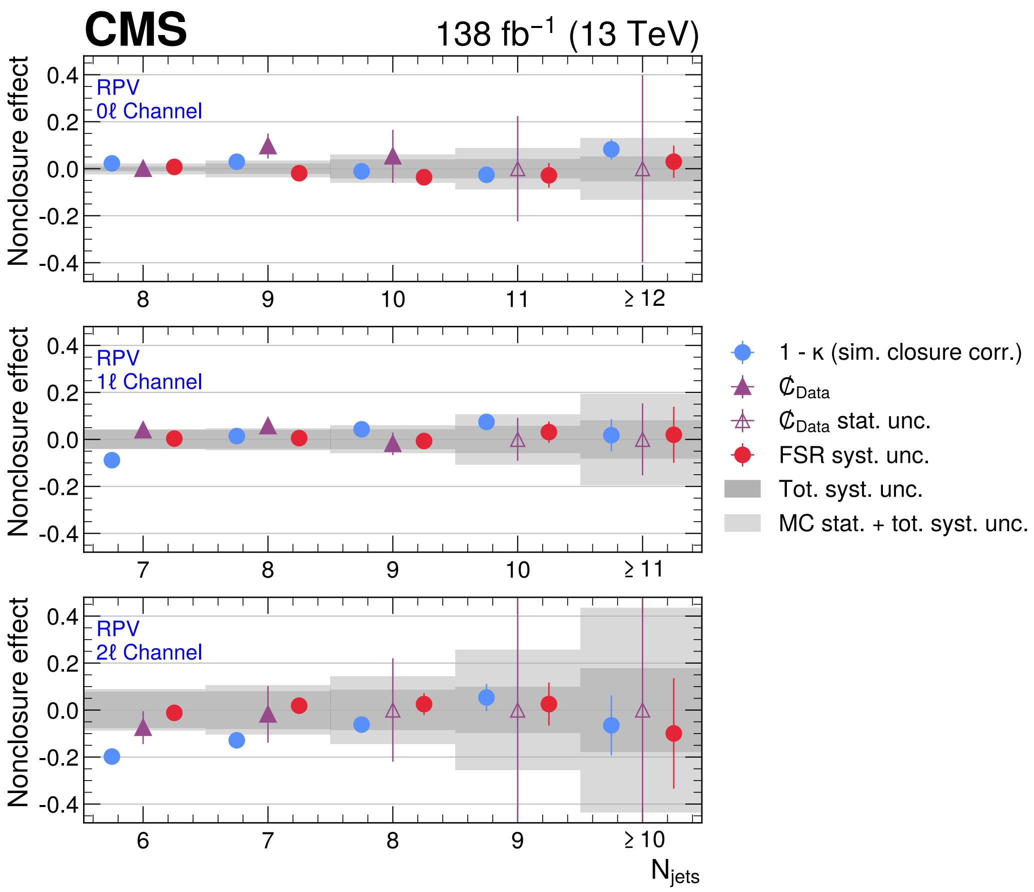

Figure 4: One minus the simulation-based closure correction κ (blue circle), the residual nonclosure $\mathcal{C}$ in data (solid purple triangle), and the FSR systematic uncertainty (red circle) are shown for each N_{jets} category for the 0ℓ (upper), 1ℓ (middle), and 2ℓ (lower panel) channels. All values correspond to the low-mass optimization for the RPV signal model. The value of $\mathcal{C}$ shown is the maximum value of the stepping procedure described in the text. Note the data-based nonclosure systematic uncertainty is defined to be the nonclosure in the lowest N_{jets} bin for each of the channels. Open purple triangles show the statistical uncertainty in $\mathcal{C}$ in data for categories in which all VR and ABCD boundaries have a signal fraction exceeding 5%. All data-based nonclosure values are calculated after applying the simulation-based closure correction, such that an observed nonclosure of zero signifies identical modeling of the $S_{\text{NN},1}$-$S_{\text{NN},2}$ correlation in simulation and data.

than the typical size of the uncertainties, as seen in the figure for the 2ℓ channel, indicating that the simulation models the data well for any residual $S_{\text{NN},1}$-$S_{\text{NN},2}$ correlations. Across all channels and optimizations, the largest κ factor has a value of 1.887 and is found for the RPV 0ℓ channel high-mass optimization, resulting in a value of only 8% for the data-based nonclosure systematic uncertainty.

For minor background processes and signal, systematic uncertainties are estimated to account for both physical mismodeling of events and detector effects. These include uncertainties in JES and JER [75], PDFs, b and t tagging efficiencies and misidentification rates, lepton identification, trigger efficiencies, pileup, renormalization and factorization scales (μ_{R}, μ_{F}), the integrated luminosity [20–22], and in the correction factor for the ECAL timing shift [25], referred to as trigger prefiring. These uncertainties are applied to each of the analysis regions to allow for adjustments in the normalization and shape of each of these processes. All systematic uncertainties originating from the same source are correlated across all N_{jets} and ABCD bins, search channels, and processes. Minor background processes normalizations are assigned an additional 20% uncertainty to account for discrepancies between LO and NLO cross section calculations [76].

Table 3 shows the relative size of each systematic uncertainty in the expected event yield for the background and signal processes across the three search channels for the RPV SUSY model and the ABCD boundaries optimized for low $m_{\tilde{t}}$. The ranges shown for each systematic uncertainty account for the difference in their value across N_{jets} categories and ABCD regions.

Table 3: Magnitude of systematic uncertainties for the 0ℓ, 1ℓ, and 2ℓ channels based on the RPV-trained NN and ABCD bin boundaries optimized for low $m_{\tilde{t}}$. Reported values are in units of % and ranges correspond to the 16th and 84th percentile for the value of a systematic uncertainty across all applicable analysis regions (ABCD regions and N_{jets} categories). The maximum value for a given systematic uncertainty across these regions is shown in parentheses. Other backgrounds include the QCD multijet and minor background processes. The RPV signal model used assumes $m_{\tilde{t}} = 550$ GeV. The systematic uncertainties based on the RPV-trained model are representative of the values obtained for the stealth SY$\overline{\text{Y}}$-trained model.

Source of		0ℓ			1ℓ			2ℓ	
uncertainty (%)	$t\bar{t}$	Other	RPV signal	$t\bar{t}$	Other	RPV signal	$t\bar{t}$	Other	RPV signal
PDF	—	<1 (1)	<1	—	<1 (1)	<1	—	<1 (2)	<1
(μ_R, μ_F) scales	—	1–8 (16)	0–1 (2)	—	0–5 (13)	0–1 (2)	—	0–7 (19)	0–1 (2)
FSR	1–3 (3)	1–14 (56)	1–12 (18)	0–1 (3)	1–12 (26)	1–7 (15)	0–6 (9)	2–21 (100)	1–9 (16)
ISR	—	0–10 (17)	1–4 (5)	—	0–8 (15)	1–4 (5)	—	3–11 (17)	0–4 (5)
Pileup	—	0–2 (12)	0–1 (3)	—	0–1 (22)	<1 (3)	—	0–9 (26)	0–1 (9)
ABCD nonclosure	3	—	—	5	—	—	7	—	—
κ stat. unc.	1–4 (7)	—	—	1–7 (8)	—	—	5–15 (19)	—	—
QCD transfer factor	—	1–4 (16)	—	—	<1 (1)	—	—	<1	—
JES	—	4–18 (100)	0–10 (27)	—	1–18 (100)	1–14 (19)	—	4–100 (100)	1–15 (25)
JER	—	0–8 (23)	0–2 (4)	—	0–5 (35)	0–1 (4)	—	0–20 (45)	0–3 (9)
b tagging	—	0–1 (7)	1–2 (3)	—	0–1 (3)	<1	—	0–1 (7)	<1 (2)
t tagging	—	26–33 (42)	26–31 (34)	—	—	—	—	—	—
Jet trigger	—	0–1 (1)	<1 (1)	—	—	—	—	—	—
Lepton ID	—	—	—	—	3–3 (4)	3–3 (3)	—	5–6 (6)	5–5 (6)
Trigger prefiring	—	0–2 (7)	0–2 (3)	—	0–3 (6)	0–3 (4)	—	0–3 (11)	0–2 (4)
Integrated lumi.	—	1.6	1.6	—	1.6	1.6	—	1.6	1.6
Theor. cross section	—	20	—	—	20	—	—	20	—

8 Results and interpretation

The fit results for the full Run 2 data with the signal strength fixed to zero (background-only fit) are shown in Fig. 5 for the RPV signal model with ABCD boundaries optimized for low $m_{\tilde{t}}$. The results for the stealth SY$\overline{\text{Y}}$ model and the high-mass optimization are shown in Appendix A. Ratios of numbers of observed data and predicted events as a function of N_{jets} are shown in the lower panel with error bars representing the systematic and statistical uncertainties. Overall, good agreement is observed between the data and the prediction; no excess of events is observed.

The data are used to place 95% confidence level (CL) upper limits on the signal cross section $\sigma_{\tilde{t}\bar{\tilde{t}}}$ for both the RPV and stealth SY$\overline{\text{Y}}$ SUSY models according to the CL_s criterion [77, 78] with an LHC-style likelihood ratio [79] as the test statistic using the asymptotic approximation [80]. These results are determined using the CMS statistical analysis tool COMBINE [81] and assume

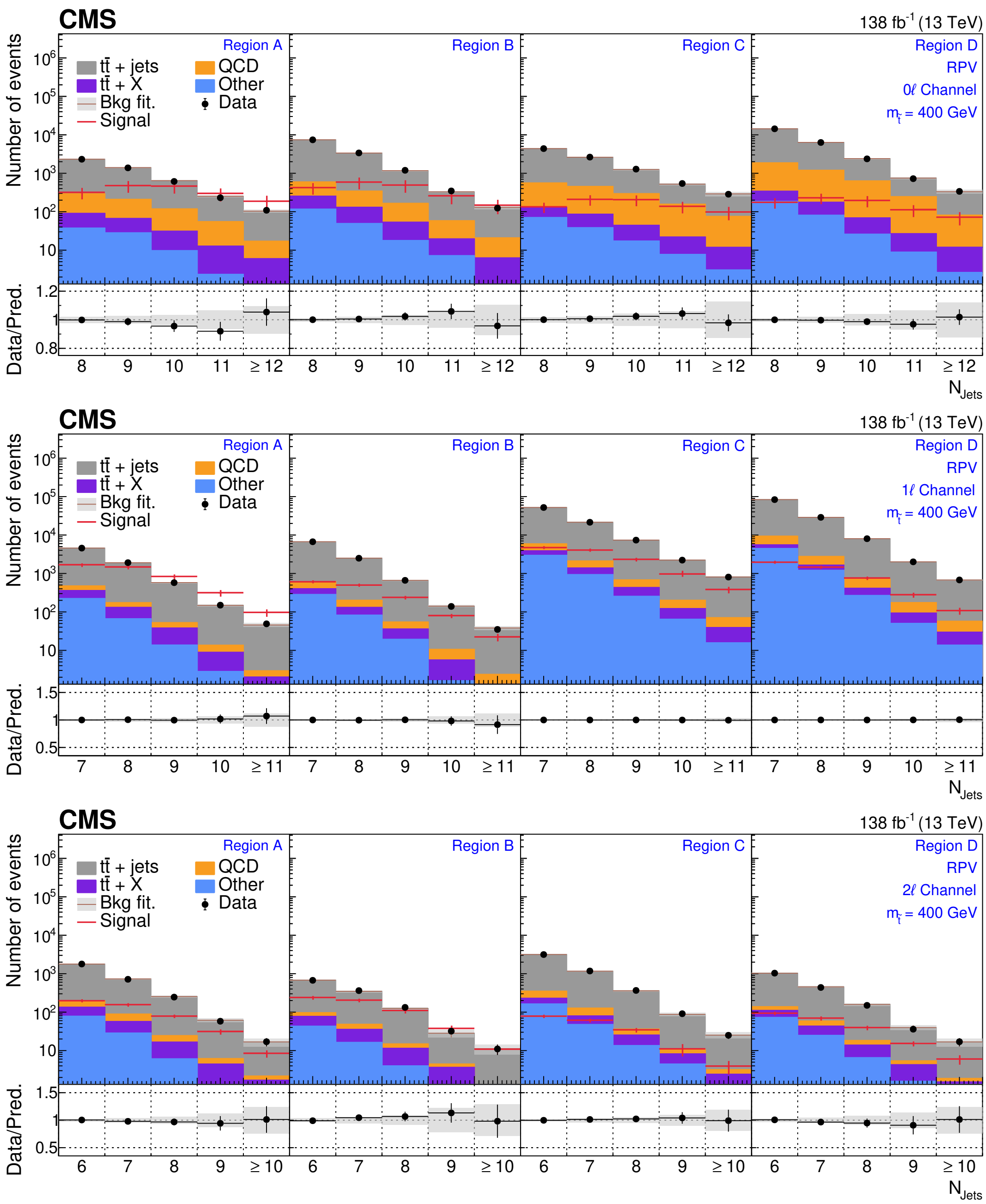

Figure 5: The N_{jets} distributions from the background-only fits to data. Fits are run with the signal strength fixed to zero and all background process event yields are obtained from their fit predictions. The signal distribution overlaid corresponds to the RPV model with $m_{\tilde{t}} = 400\,\text{GeV}$. The graphs in the upper, middle, and lower rows correspond to the 0ℓ, 1ℓ, and 2ℓ channels, respectively. The four panels in each row show the N_{jets} distributions for the A, B, C, and D regions (left to right). The gray error band shows the combined statistical and systematic uncertainty from the background-only fit distributions.

100% branching fraction to the considered $\widetilde{t}$ squark decay. The low-mass ABCD boundaries are used for the RPV (stealth $SY\overline{Y}$) signal models with $m_{\widetilde{t}} < 625\,(675)$ GeV, with the high-mass boundaries used for higher $m_{\widetilde{t}}$. Figures 6 and 7 show the expected and observed upper limit on $\sigma_{\widetilde{t}\overline{\widetilde{t}}}$ for the RPV and stealth $SY\overline{Y}$ models with $m_{\widetilde{t}}$ ranging from 300 to 1250 GeV for each lepton channel separately and for all three channels combined, respectively. The theoretical cross section is also shown along with its uncertainty. Based on the results from the combination of all channels, $\widetilde{t}$ squark masses up to 700 GeV are excluded for the RPV model and up to 930 GeV for the stealth $SY\overline{Y}$ model.

9 Summary

A search for the pair production of top squarks with decays to top quarks and six additional gluons or light-flavor quarks via R-parity violating (RPV) or stealth $SY\overline{Y}$ supersymmetric decays is presented. The search is performed using proton-proton collision events at $\sqrt{s} = 13$ TeV, corresponding to an integrated luminosity of 138 fb^{-1}, collected by the CMS detector in 2016–2018. Events are selected in three search channels, defined as having at least six jets and zero, one, or two electrons or muons. No requirement is placed on the presence of missing transverse momentum.

This analysis is an extension of a previous search for these signatures [16], which observed a deviation with a local significance of 2.8 standard deviations for a top squark mass of 400 GeV for the RPV model. The main improvements of this search are the addition of the zero- and two-lepton channels as well as the inclusion of a novel, neural-network-based background estimation method referred to as ABCDisCoTEC [17]. The key feature of this new method is the creation of two uncorrelated neural network variables that can be used with an ABCD-style background estimation method. The backgrounds are estimated from a simultaneous binned likelihood fit to all search channels in several categories of jet multiplicity, with the contribution from the main $t\overline{t}$ + jets background constrained via the ABCD relationship that encodes the independence between the two neural network variables. This new background estimation method, compared to that of Ref. [16], reduces the dependence of the analysis on uncertainties related to the modeling of the jet multiplicity spectrum. With this alternate background estimation technique, we achieve an improvement in signal sensitivity at low top squark mass. For example, the expected upper limit on the production cross section improves by a factor of 1.53 for a top squark mass of 400 GeV for the RPV model. Overall, good agreement between the data and the background prediction is observed, and the deviation observed previously is not confirmed.

The results are interpreted using two top squark decay topologies that generate signatures with low missing transverse momentum: the RPV and stealth $SY\overline{Y}$ models. For the RPV model with top squark decays to a top quark and neutralino, with the subsequent decay of the neutralino to three light-flavored quarks, top squark masses up to 700 GeV are excluded at 95% confidence level. Similarly, top squark masses of up to 930 GeV are excluded in the context of the stealth $SY\overline{Y}$ model where top squarks decay to a top quark, gluons, and a soft gravitino via a hidden sector.

Acknowledgments

We congratulate our colleagues in the CERN accelerator departments for the excellent performance of the LHC and thank the technical and administrative staffs at CERN and at other

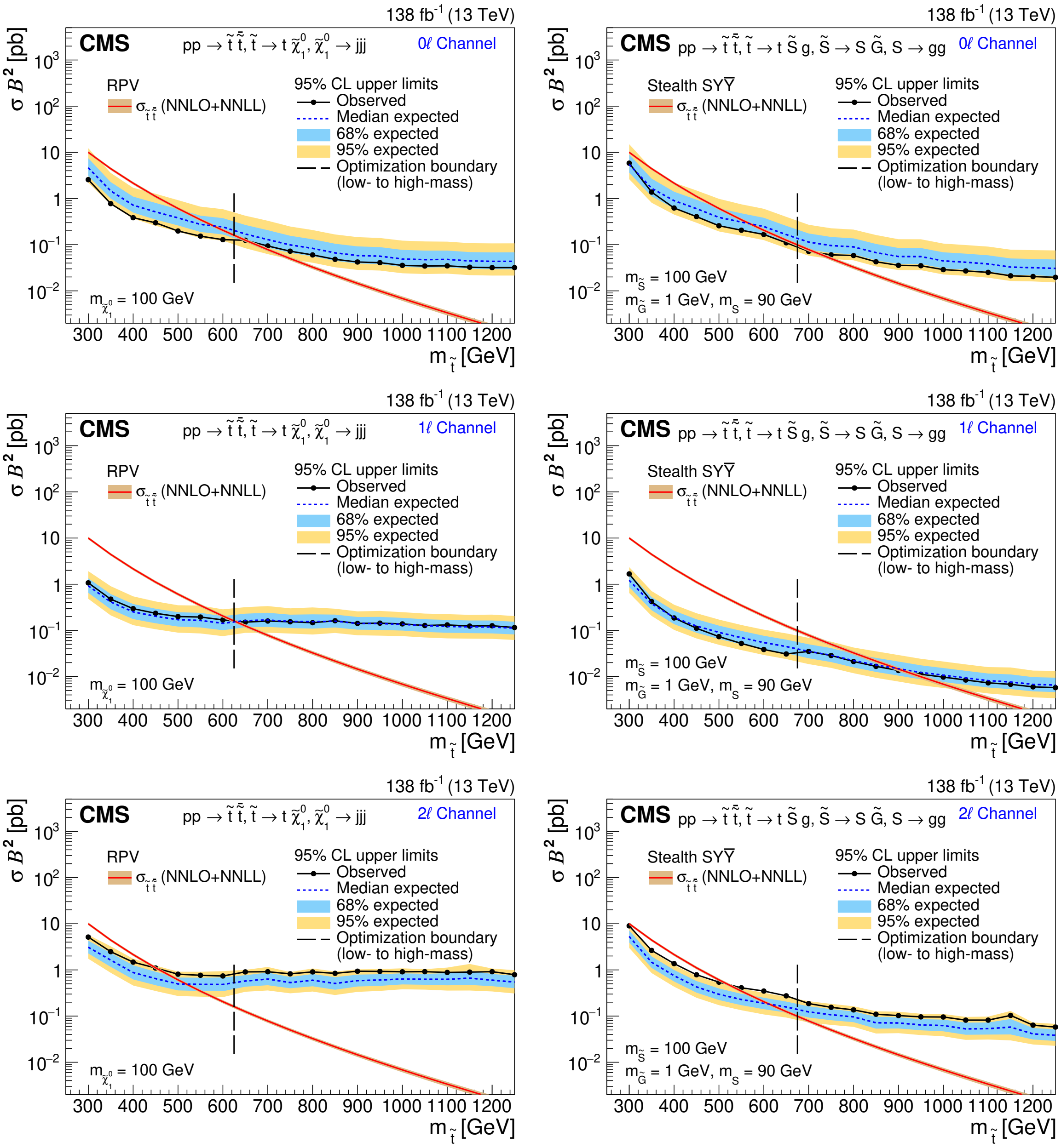

Figure 6: The 95% CL upper limit on $\sigma_{\tilde{t}\bar{\tilde{t}}}$ for the RPV (left) and stealth SY$\bar{\text{Y}}$ (right) SUSY signal models as a function of $m_{\tilde{t}}$ for the 0ℓ channel (upper), 1ℓ channel (middle), and 2ℓ channel (lower), assuming 100% branching fraction to the considered $\tilde{t}$ squark decay. The median expected limit is shown in the dashed blue line, with the 68 and 95% intervals shown in light-blue and yellow, respectively. The observed limit is shown in black. The vertical dashed line denotes the transition from the low- to high-mass optimization ABCD boundaries. Additionally, the theoretical cross section is shown in red with its uncertainty in light brown.

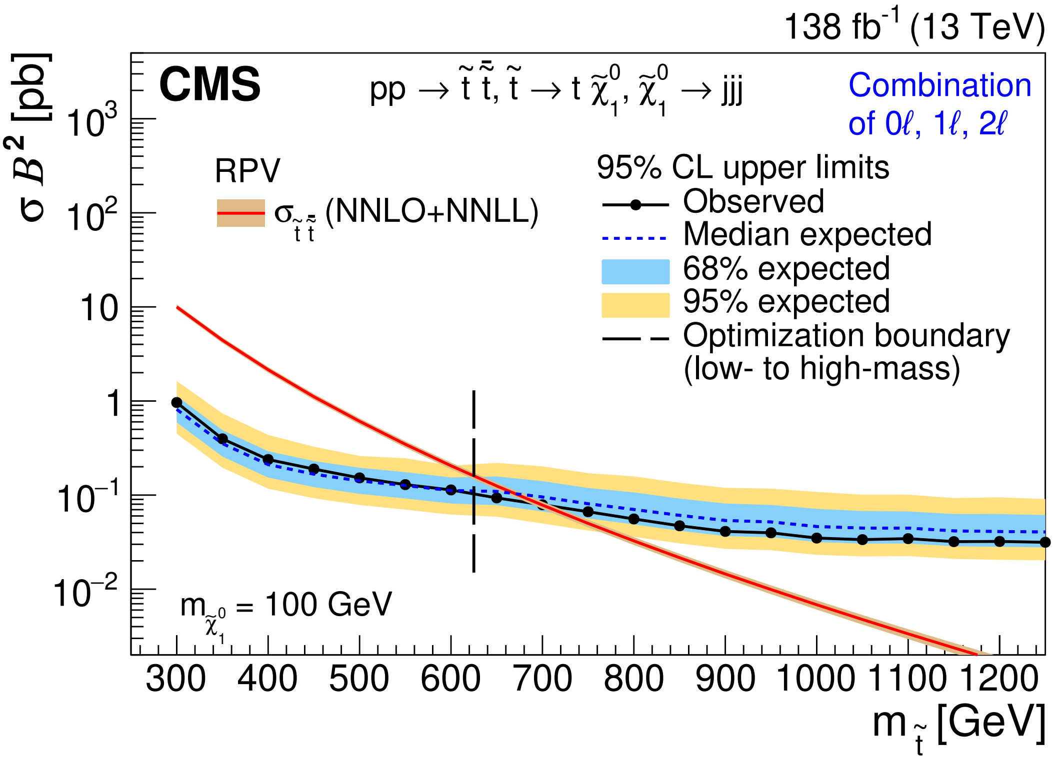

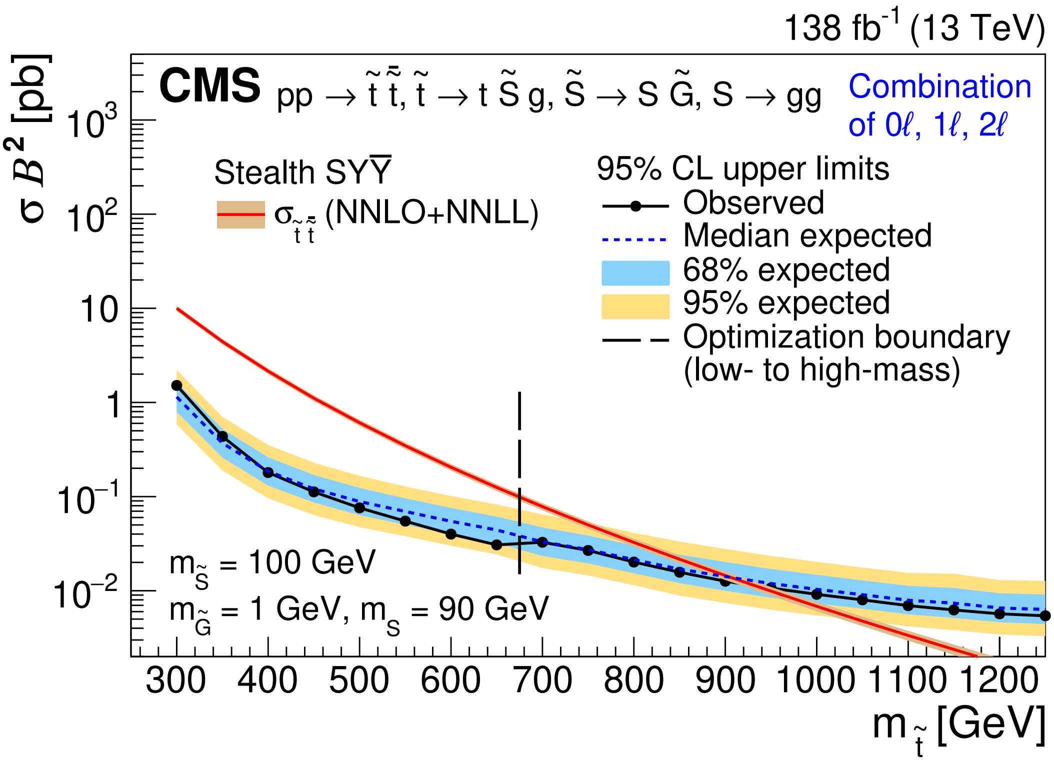

Figure 7: Observed and expected upper limits at 95% CL on $\sigma_{\tilde{t}\bar{\tilde{t}}}$ for the RPV (upper) and stealth SY$\overline{\text{Y}}$ (lower) SUSY signal models as functions of $m_{\tilde{t}}$ for the combination of all three channels, assuming 100% branching fraction to the considered $\tilde{t}$ squark decay. The median expected limit is shown in the dashed blue line, with the 68 and 95% intervals shown in light blue and yellow, respectively. The observed limit is shown in black. The vertical dashed line denotes the transition from the low- to high-mass optimization ABCD boundaries. Additionally, the theoretical cross section is shown in red with its uncertainty in light brown.

CMS institutes for their contributions to the success of the CMS effort. In addition, we gratefully acknowledge the computing centers and personnel of the Worldwide LHC Computing Grid and other centers for delivering so effectively the computing infrastructure essential to our analyses. Finally, we acknowledge the enduring support for the construction and operation of the LHC, the CMS detector, and the supporting computing infrastructure provided by the following funding agencies: SC (Armenia), BMBWF and FWF (Austria); FNRS and FWO (Belgium); CNPq, CAPES, FAPERJ, FAPERGS, and FAPESP (Brazil); MES and BNSF (Bulgaria); CERN; CAS, MoST, and NSFC (China); MINCIENCIAS (Colombia); MSES and CSF (Croatia); RIF (Cyprus); SENESCYT (Ecuador); ERC PRG, RVTT3 and MoER TK202 (Estonia); Academy of Finland, MEC, and HIP (Finland); CEA and CNRS/IN2P3 (France); SRNSF (Georgia); BMBF, DFG, and HGF (Germany); GSRI (Greece); NKFIH (Hungary); DAE and DST (India); IPM (Iran); SFI (Ireland); INFN (Italy); MSIP and NRF (Republic of Korea); MES (Latvia); LMTLT (Lithuania); MOE and UM (Malaysia); BUAP, CINVESTAV, CONACYT, LNS, SEP, and UASLP-FAI (Mexico); MOS (Montenegro); MBIE (New Zealand); PAEC (Pakistan); MES and NSC (Poland); FCT (Portugal); MESTD (Serbia); MICIU/AEI and PCTI (Spain); MOSTR (Sri Lanka); Swiss Funding Agencies (Switzerland); MST (Taipei); MHESI and NSTDA (Thailand); TUBITAK and TENMAK (Turkey); NASU (Ukraine); STFC (United Kingdom); DOE and NSF (USA).

Individuals have received support from the Marie-Curie program and the European Research Council and Horizon 2020 Grant, contract Nos. 675440, 724704, 752730, 758316, 765710, 824093, 101115353, 101002207, 101001205, and COST Action CA16108 (European Union); the Leventis Foundation; the Alfred P. Sloan Foundation; the Alexander von Humboldt Foundation; the Science Committee, project no. 22rl-037 (Armenia); the Fonds pour la Formation à la Recherche dans l'Industrie et dans l'Agriculture (FRIA-Belgium); the Beijing Municipal Science & Technology Commission, No. Z191100007219010, the Fundamental Research Funds for the Central Universities, the Ministry of Science and Technology of China under Grant No. 2023YFA1605804, and the Natural Science Foundation of China under Grant No. 12061141002 (China); the Ministry of Education, Youth and Sports (MEYS) of the Czech Republic; the Shota Rustaveli National Science Foundation, grant FR-22-985 (Georgia); the Deutsche Forschungsgemeinschaft (DFG), among others, under Germany's Excellence Strategy – EXC 2121 "Quantum Universe" – 390833306, and under project number 400140256 - GRK2497; the Hellenic Foundation for Research and Innovation (HFRI), Project Number 2288 (Greece); the Hungarian Academy of Sciences, the New National Excellence Program - ÚNKP, the NKFIH research grants K 131991, K 133046, K 138136, K 143460, K 143477, K 146913, K 146914, K 147048, 2020-2.2.1-ED-2021-00181, TKP2021-NKTA-64, and 2021-4.1.2-NEMZ_KI-2024-00036 (Hungary); the Council of Science and Industrial Research, India; ICSC – National Research Center for High Performance Computing, Big Data and Quantum Computing and FAIR – Future Artificial Intelligence Research, funded by the NextGenerationEU program (Italy); the Latvian Council of Science; the Ministry of Education and Science, project no. 2022/WK/14, and the National Science Center, contracts Opus 2021/41/B/ST2/01369 and 2021/43/B/ST2/01552 (Poland); the Fundação para a Ciência e a Tecnologia, grant CEECIND/01334/2018 (Portugal); the National Priorities Research Program by Qatar National Research Fund; MICIU/AEI/10.13039/501100011033, ERDF/EU, "European Union NextGenerationEU/PRTR", and Programa Severo Ochoa del Principado de Asturias (Spain); the Chulalongkorn Academic into Its 2nd Century Project Advancement Project, and the National Science, Research and Innovation Fund via the Program Management Unit for Human Resources & Institutional Development, Research and Innovation, grant B39G680009 (Thailand); the Kavli Foundation; the Nvidia Corporation; the SuperMicro Corporation; the Welch Foundation, contract C-1845; and the Weston Havens Foundation (USA).

References

[1] P. Fayet and S. Ferrara, “Supersymmetry”, *Phys. Rept.* **32** (1977) 249, doi:10.1016/0370-1573(77)90066-7.

[2] S. P. Martin, “A supersymmetry primer”, *Adv. Ser. Direct. High Energy Phys.* **21** (1997) 1, doi:10.1142/9789812839657_0001, arXiv:hep-ph/9709356.

[3] CMS Collaboration, “Search for direct top squark pair production in events with one lepton, jets, and missing transverse momentum at 13 TeV with the CMS experiment”, *JHEP* **05** (2020) 032, doi:10.1007/JHEP05(2020)032, arXiv:1912.08887.

[4] CMS Collaboration, “Search for supersymmetry in proton-proton collisions at 13 TeV in final states with jets and missing transverse momentum”, *JHEP* **10** (2019) 244, doi:10.1007/JHEP10(2019)244, arXiv:1908.04722.

[5] CMS Collaboration, “Searches for physics beyond the standard model with the M_{T2} variable in hadronic final states with and without disappearing tracks in proton-proton collisions at $\sqrt{s} = 13$ TeV”, *Eur. Phys. J. C* **80** (2020) 3, doi:10.1140/epjc/s10052-019-7493-x, arXiv:1909.03460.

[6] CMS Collaboration, “Search for top squark production in fully-hadronic final states in proton-proton collisions at $\sqrt{s} = 13$ TeV”, *Phys. Rev. D* **104** (2021) 052001, doi:10.1103/PhysRevD.104.052001, arXiv:2103.01290.

[7] ATLAS Collaboration, “Search for a scalar partner of the top quark in the all-hadronic $t\bar{t}$ plus missing transverse momentum final state at $\sqrt{s} = 13$ TeV with the ATLAS detector”, *Eur. Phys. J. C* **80** (2020) 737, doi:10.1140/epjc/s10052-020-8102-8, arXiv:2004.14060.

[8] ATLAS Collaboration, “Search for new phenomena with top quark pairs in final states with one lepton, jets, and missing transverse momentum in pp collisions at $\sqrt{s}$ = 13 TeV with the ATLAS detector”, *JHEP* **04** (2021) 174, doi:10.1007/JHEP04(2021)174, arXiv:2012.03799.

[9] ATLAS Collaboration, “Search for new phenomena in events with two opposite-charge leptons, jets and missing transverse momentum in pp collisions at $\sqrt{\mathrm{s}}$ = 13 TeV with the ATLAS detector”, *JHEP* **04** (2021) 165, doi:10.1007/JHEP04(2021)165, arXiv:2102.01444.

[10] ATLAS Collaboration, “Search for new phenomena with top-quark pairs and large missing transverse momentum using 140 fb^{-1} of pp collision data at $\sqrt{s}$ = 13 TeV with the ATLAS detector”, *JHEP* **03** (2024) 139, doi:10.1007/JHEP03(2024)139, arXiv:2401.13430.

[11] R. Barbier et al., “R-parity violating supersymmetry”, *Phys. Rept.* **420** (2005) 1, doi:10.1016/j.physrep.2005.08.006, arXiv:hep-ph/0406039.

[12] H. K. Dreiner and G. G. Ross, “R-parity violation at hadron colliders”, *Nucl. Phys. B* **365** (1991) 597, doi:10.1016/0550-3213(91)90443-2.

[13] J. Fan, M. Reece, and J. T. Ruderman, “Stealth supersymmetry”, *JHEP* **11** (2011) 012, doi:10.1007/JHEP11(2011)012, arXiv:1105.5135.

[14] J. Fan, M. Reece, and J. T. Ruderman, "A stealth supersymmetry sampler", *JHEP* **07** (2012) 196, doi:10.1007/JHEP07(2012)196, arXiv:1201.4875.

[15] J. Fan et al., "Stealth supersymmetry simplified", *JHEP* **07** (2016) 016, doi:10.1007/JHEP07(2016)016, arXiv:1512.05781.

[16] CMS Collaboration, "Search for top squarks in final states with two top quarks and several light-flavor jets in proton-proton collisions at $\sqrt{s}$ = 13 TeV", *Phys. Rev. D* **104** (2021) 032006, doi:10.1103/PhysRevD.104.032006, arXiv:2102.06976.

[17] CMS Collaboration, "Machine learning method for enforcing variable independence in background estimation with LHC data: ABCDisCoTEC", 2025. arXiv:2506.08826. Submitted to *MLST*.

[18] G. Kasieczka, B. Nachman, M. D. Schwartz, and D. Shih, "Automating the ABCD method with machine learning", *Phys. Rev. D* **103** (2021) 035021, doi:10.1103/PhysRevD.103.035021, arXiv:2007.14400.

[19] HEPData record for this analysis, 2025. doi:10.17182/hepdata.156817.

[20] CMS Collaboration, "Precision luminosity measurement in proton-proton collisions at $\sqrt{s} = 13$ TeV in 2015 and 2016 at CMS", *Eur. Phys. J. C* **81** (2021) 800, doi:10.1140/epjc/s10052-021-09538-2, arXiv:2104.01927.

[21] CMS Collaboration, "CMS luminosity measurement for the 2017 data-taking period at $\sqrt{s} = 13$ TeV", CMS Physics Analysis Summary CMS-PAS-LUM-17-004, 2018.

[22] CMS Collaboration, "CMS luminosity measurement for the 2018 data-taking period at $\sqrt{s} = 13$ TeV", CMS Physics Analysis Summary CMS-PAS-LUM-18-002, 2019.

[23] CMS Collaboration, "The CMS experiment at the CERN LHC", *JINST* **3** (2008) S08004, doi:10.1088/1748-0221/3/08/S08004.

[24] CMS Collaboration, "Development of the CMS detector for the CERN LHC Run 3", *JINST* **19** (2024) P05064, doi:10.1088/1748-0221/19/05/P05064, arXiv:2309.05466.

[25] CMS Collaboration, "Performance of the CMS Level-1 trigger in proton-proton collisions at $\sqrt{s} = 13$ TeV", *JINST* **15** (2020) P10017, doi:10.1088/1748-0221/15/10/P10017, arXiv:2006.10165.

[26] CMS Collaboration, "The CMS trigger system", *JINST* **12** (2017) P01020, doi:10.1088/1748-0221/12/01/P01020, arXiv:1609.02366.

[27] CMS Collaboration, "Performance of the CMS high-level trigger during LHC Run 2", *JINST* **19** (2024) P11021, doi:10.1088/1748-0221/19/11/P11021, arXiv:2410.17038.

[28] CMS Collaboration, "Electron and photon reconstruction and identification with the CMS experiment at the CERN LHC", *JINST* **16** (2021) P05014, doi:10.1088/1748-0221/16/05/P05014, arXiv:2012.06888.

[29] CMS Collaboration, "Performance of the CMS muon detector and muon reconstruction with proton-proton collisions at $\sqrt{s} = 13$ TeV", *JINST* **13** (2018) P06015, doi:10.1088/1748-0221/13/06/P06015, arXiv:1804.04528.

[30] CMS Collaboration, "Description and performance of track and primary-vertex reconstruction with the CMS tracker", *JINST* **9** (2014) P10009, doi:10.1088/1748-0221/9/10/P10009, arXiv:1405.6569.

[31] CMS Collaboration, "Technical proposal for the Phase-II upgrade of the Compact Muon Solenoid", CMS Technical Proposal CERN-LHCC-2015-010, CMS-TDR-15-02, 2015.

[32] CMS Collaboration, "Particle-flow reconstruction and global event description with the CMS detector", *JINST* **12** (2017) P10003, doi:10.1088/1748-0221/12/10/P10003, arXiv:1706.04965.

[33] M. Cacciari, G. P. Salam, and G. Soyez, "The anti-k_T jet clustering algorithm", *JHEP* **04** (2008) 063, doi:10.1088/1126-6708/2008/04/063, arXiv:0802.1189.

[34] M. Cacciari, G. P. Salam, and G. Soyez, "FastJet user manual", *Eur. Phys. J. C* **72** (2012) 1896, doi:10.1140/epjc/s10052-012-1896-2, arXiv:1111.6097.

[35] CMS Collaboration, "Pileup mitigation at CMS in 13 TeV data", *JINST* **15** (2020) P09018, doi:10.1088/1748-0221/15/09/P09018, arXiv:2003.00503.

[36] CMS Collaboration, "Jet energy scale and resolution in the CMS experiment in pp collisions at 8 TeV", *JINST* **12** (2017) P02014, doi:10.1088/1748-0221/12/02/P02014, arXiv:1607.03663.

[37] CMS Collaboration, "Identification of heavy-flavour jets with the CMS detector in pp collisions at 13 TeV", *JINST* **13** (2018) P05011, doi:10.1088/1748-0221/13/05/P05011, arXiv:1712.07158.

[38] E. Bols et al., "Jet flavour classification using DeepJet", *JINST* **15** (2020) P12012, doi:10.1088/1748-0221/15/12/P12012, arXiv:2008.10519.

[39] CMS Collaboration, "Performance of the DeepJet b tagging algorithm using 41.9 fb^{-1} of data from proton-proton collisions at 13 TeV with Phase 1 CMS detector", CMS Detector Performance Note CMS-DP-2018-058, 2018.

[40] CMS Collaboration, "ECAL 2016 refined calibration and Run2 summary plots", CMS Detector Performance Note CMS-DP-2020-021, 2020.

[41] K. Rehermann and B. Tweedie, "Efficient identification of boosted semileptonic top quarks at the LHC", *JHEP* **03** (2011) 059, doi:10.1007/JHEP03(2011)059, arXiv:1007.2221.

[42] P. Nason, "A new method for combining NLO QCD with shower Monte Carlo algorithms", *JHEP* **11** (2004) 040, doi:10.1088/1126-6708/2004/11/040, arXiv:hep-ph/0409146.

[43] S. Frixione, P. Nason, and C. Oleari, "Matching NLO QCD computations with parton shower simulations: the POWHEG method", *JHEP* **11** (2007) 070, doi:10.1088/1126-6708/2007/11/070, arXiv:0709.2092.

[44] S. Alioli, P. Nason, C. Oleari, and E. Re, "A general framework for implementing NLO calculations in shower Monte Carlo programs: the POWHEG BOX", *JHEP* **06** (2010) 043, doi:10.1007/JHEP06(2010)043, arXiv:1002.2581.

[45] S. Frixione, P. Nason, and G. Ridolfi, "A positive-weight next-to-leading-order Monte Carlo for heavy flavour hadroproduction", *JHEP* **09** (2007) 126, doi:10.1088/1126-6708/2007/09/126, arXiv:0707.3088.

[46] E. Re, "Single-top Wt-channel production matched with parton showers using the POWHEG method", *Eur. Phys. J. C* **71** (2011) 1547, doi:10.1140/epjc/s10052-011-1547-z, arXiv:1009.2450.

[47] S. Alioli, P. Nason, C. Oleari, and E. Re, "NLO single-top production matched with shower in POWHEG: s- and t-channel contributions", *JHEP* **09** (2009) 111, doi:10.1088/1126-6708/2009/09/111, arXiv:0907.4076. [Erratum: doi:10.1007/JHEP02(2010)011].

[48] J. Alwall et al., "The automated computation of tree-level and next-to-leading order differential cross sections, and their matching to parton shower simulations", *JHEP* **07** (2014) 079, doi:10.1007/JHEP07(2014)079, arXiv:1405.0301.

[49] T. Sjöstrand et al., "An introduction to PYTHIA 8.2", *Comput. Phys. Commun.* **191** (2015) 159, doi:10.1016/j.cpc.2015.01.024, arXiv:1410.3012.

[50] M. Czakon and A. Mitov, "Top++: A program for the calculation of the top-pair cross-section at hadron colliders", *Comput. Phys. Commun.* **185** (2014) 2930, doi:10.1016/j.cpc.2014.06.021, arXiv:1112.5675.

[51] P. Kant et al., "HATHOR for single top-quark production: Updated predictions and uncertainty estimates for single top-quark production in hadronic collisions", *Comput. Phys. Commun.* **191** (2015) 74, doi:10.1016/j.cpc.2015.02.001, arXiv:1406.4403.

[52] M. Aliev et al., "HATHOR: HAdronic Top and Heavy quarks crOss section calculatoR", *Comput. Phys. Commun.* **182** (2011) 1034, doi:10.1016/j.cpc.2010.12.040, arXiv:1007.1327.

[53] T. Gehrmann et al., "W^+W^- production at hadron colliders in next to next to leading order QCD", *Phys. Rev. Lett.* **113** (2014) 212001, doi:10.1103/PhysRevLett.113.212001, arXiv:1408.5243.

[54] J. M. Campbell and R. K. Ellis, "An update on vector boson pair production at hadron colliders", *Phys. Rev. D* **60** (1999) 113006, doi:10.1103/PhysRevD.60.113006, arXiv:hep-ph/9905386.

[55] J. M. Campbell, R. K. Ellis, and C. Williams, "Vector boson pair production at the LHC", *JHEP* **07** (2011) 018, doi:10.1007/JHEP07(2011)018, arXiv:1105.0020.

[56] Y. Li and F. Petriello, "Combining QCD and electroweak corrections to dilepton production in FEWZ", *Phys. Rev. D* **86** (2012) 094034, doi:10.1103/PhysRevD.86.094034, arXiv:1208.5967.

[57] C. Borschensky et al., "Squark and gluino production cross sections in pp collisions at $\sqrt{s} = 13, 14, 33$ and 100 TeV", *Eur. Phys. J. C* **74** (2014) 3174, doi:10.1140/epjc/s10052-014-3174-y, arXiv:1407.5066.

[58] W. Beenakker et al., "NNLL-fast: predictions for coloured supersymmetric particle production at the LHC with threshold and Coulomb resummation", *JHEP* **12** (2016) 133, doi:10.1007/JHEP12(2016)133, arXiv:1607.07741.

[59] W. Beenakker et al., “NNLL resummation for stop pair-production at the LHC”, *JHEP* **05** (2016) 153, doi:10.1007/JHEP05(2016)153, arXiv:1601.02954.

[60] W. Beenakker et al., “Supersymmetric top and bottom squark production at hadron colliders”, *JHEP* **08** (2010) 098, doi:10.1007/JHEP08(2010)098, arXiv:1006.4771.

[61] W. Beenakker et al., “Stop production at hadron colliders”, *Nucl. Phys. B* **515** (1998) 3, doi:10.1016/S0550-3213(98)00014-5, arXiv:hep-ph/9710451.

[62] CMS Collaboration, “Extraction and validation of a new set of CMS PYTHIA8 tunes from underlying-event measurements”, *Eur. Phys. J. C* **80** (2020) 4, doi:10.1140/epjc/s10052-019-7499-4, arXiv:1903.12179.

[63] CMS Collaboration, “CMS PYTHIA 8 colour reconnection tunes based on underlying-event data”, *Eur. Phys. J. C* **83** (2023) 587, doi:10.1140/epjc/s10052-023-11630-8, arXiv:2205.02905.

[64] NNPDF Collaboration, “Parton distributions from high-precision collider data”, *Eur. Phys. J. C* **77** (2017) 663, doi:10.1140/epjc/s10052-017-5199-5, arXiv:1706.00428.

[65] GEANT4 Collaboration, “GEANT4—a simulation toolkit”, *Nucl. Instrum. Meth. A* **506** (2003) 250, doi:10.1016/S0168-9002(03)01368-8.

[66] CMS Collaboration, “Identification of heavy, energetic, hadronically decaying particles using machine-learning techniques”, *JINST* **15** (2020) P06005, doi:10.1088/1748-0221/15/06/P06005, arXiv:2004.08262.

[67] D0 Collaboration, “Search for high mass top quark production in $p\bar{p}$ collisions at $\sqrt{s} = 1.8$ TeV”, *Phys. Rev. Lett.* **74** (1995) 2422, doi:10.1103/PhysRevLett.74.2422, arXiv:hep-ex/9411001.

[68] O. Behnke, K. Kröninger, G. Schott, and T. Schörner-Sadenius, “Data analysis in high energy physics: a practical guide to statistical methods”. Wiley-VCH, 2013. doi:10.1002/9783527653416.

[69] G. J. Székely and M. L. Rizzo, “Partial distance correlation with methods for dissimilarities”, *Ann. Statist.* **42** (2014) 2382, doi:10.1214/14-AOS1255, arXiv:1310.2926.

[70] S. Odaka, N. Watanabe, and Y. Kurihara, “ME–PS matching in the simulation of multi-jet production in hadron collisions using a subtraction method”, *PTEP* **2015** (2015) 053B04, doi:10.1093/ptep/ptv059, arXiv:1409.3334.

[71] G. C. Fox and S. Wolfram, “Observables for the analysis of event shapes in e^+e^- annihilation and other processes”, *Phys. Rev. Lett.* **41** (1978) 1581, doi:10.1103/PhysRevLett.41.1581.

[72] J. D. Bjorken and S. J. Brodsky, “Statistical model for electron-positron annihilation into hadrons”, *Phys. Rev. D* **1** (1970) 1416, doi:10.1103/PhysRevD.1.1416.

[73] CMS Collaboration, “Search for supersymmetry in hadronic final states using MT2 in pp collisions at $\sqrt{s} = 7$ TeV”, *JHEP* **10** (2012) 018, doi:10.1007/JHEP10(2012)018, arXiv:1207.1798.

[74] CMS Collaboration, “CMS technical design report, volume II: Physics performance”, *J. Phys. G* **34** (2007) 995, doi:10.1088/0954-3899/34/6/S01.

[75] CMS Collaboration, “Determination of jet energy calibration and transverse momentum resolution in CMS”, *JINST* **6** (2011) P11002, doi:10.1088/1748-0221/6/11/P11002, arXiv:1107.4277.

[76] D. Kim et al., “A panoramic study of k-factors for 111 processes at the 14 TeV LHC”, *J. Korean Phys. Soc.* **84** (2024) 914, doi:10.1007/s40042-024-01072-0, arXiv:2402.16276.

[77] A. L. Read, “Presentation of search results: The CL_s technique”, *J. Phys. G* **28** (2002) 2693, doi:10.1088/0954-3899/28/10/313.

[78] T. Junk, “Confidence level computation for combining searches with small statistics”, *Nucl. Instrum. Meth. A* **434** (1999) 435, doi:10.1016/S0168-9002(99)00498-2, arXiv:hep-ex/9902006.

[79] ATLAS and CMS Collaborations, and LHC Higgs Combination Group, “Procedure for the LHC Higgs boson search combination in Summer 2011”, Technical Report CMS-NOTE-2011-005, ATL-PHYS-PUB-2011-11, 2011.

[80] G. Cowan, K. Cranmer, E. Gross, and O. Vitells, “Asymptotic formulae for likelihood-based tests of new physics”, *Eur. Phys. J. C* **71** (2011) 1554, doi:10.1140/epjc/s10052-011-1554-0, arXiv:1007.1727. [Erratum: doi:10.1140/epjc/s10052-013-2501-z].

[81] CMS Collaboration, “The CMS statistical analysis and combination tool: COMBINE”, *Comput. Softw. Big Sci.* **8** (2024) 19, doi:10.1007/s41781-024-00121-4, arXiv:2404.06614.

A Additional Figures

The background-only fit distributions shown in the main body of this work show the results of the analysis for the RPV signal model using the low-mass optimization. Figures A.1, A.2, and A.3 present the background-only fit results for the stealth $SY\overline{Y}$ analysis using the low-mass optimization as well as the background-only fits for both signal topologies using the high-mass optimization.

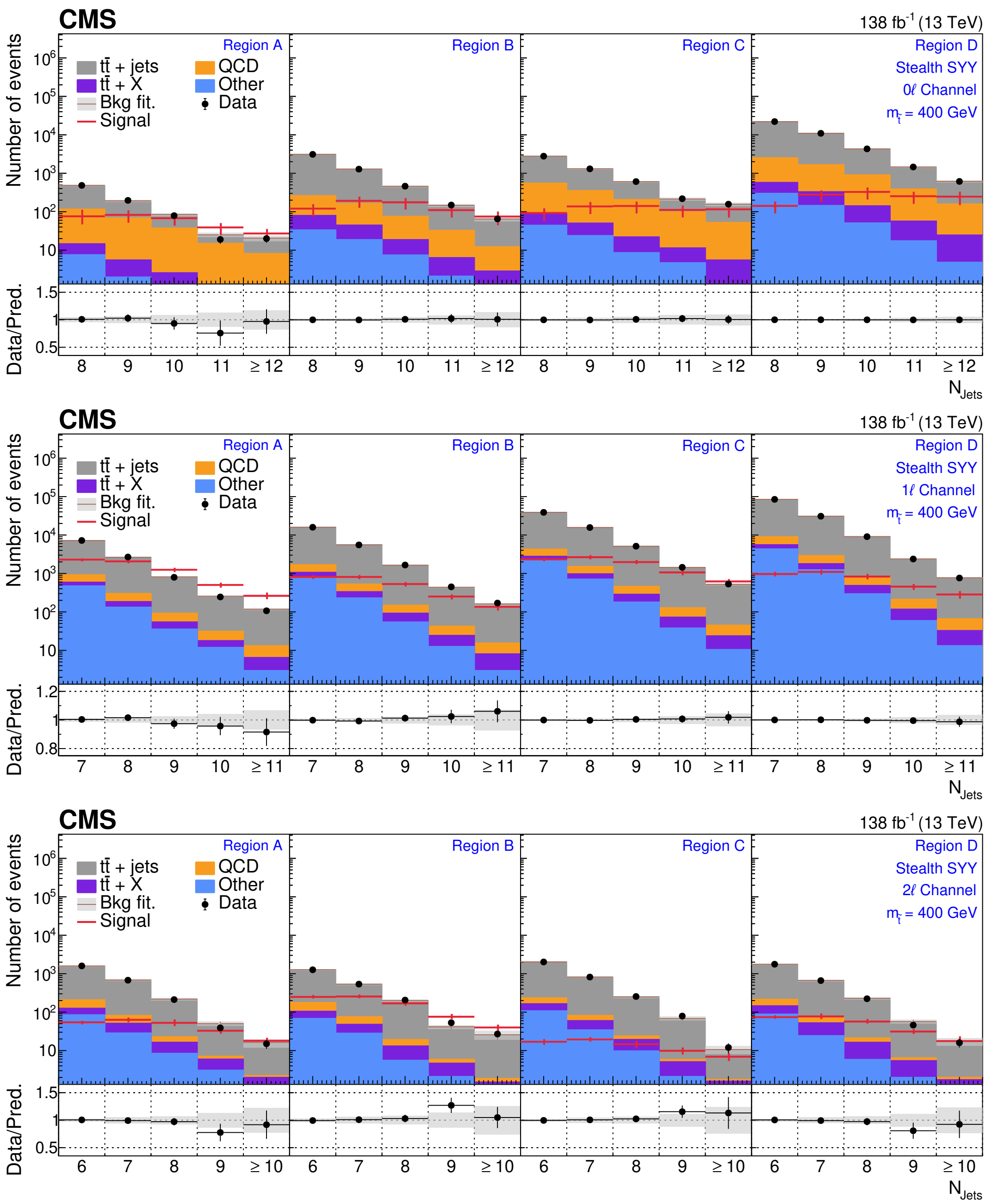

Figure A.1: The N_{jets} distributions from the background-only fits to data. Fits are run with the signal strength fixed to zero and all background process event yields are obtained from their fit predictions. The signal distribution overlaid corresponds to the stealth $SY\overline{Y}$ model with $m_{\tilde{t}} = 400\,\text{GeV}$. The graphs in the upper, middle, and lower rows correspond to the 0ℓ, 1ℓ, and 2ℓ channels, respectively. The four panels in each row show the N_{jets} distributions for the A, B, C, and D regions (left to right). The gray error band shows the combined statistical and systematic uncertainty from the background-only fit distributions.

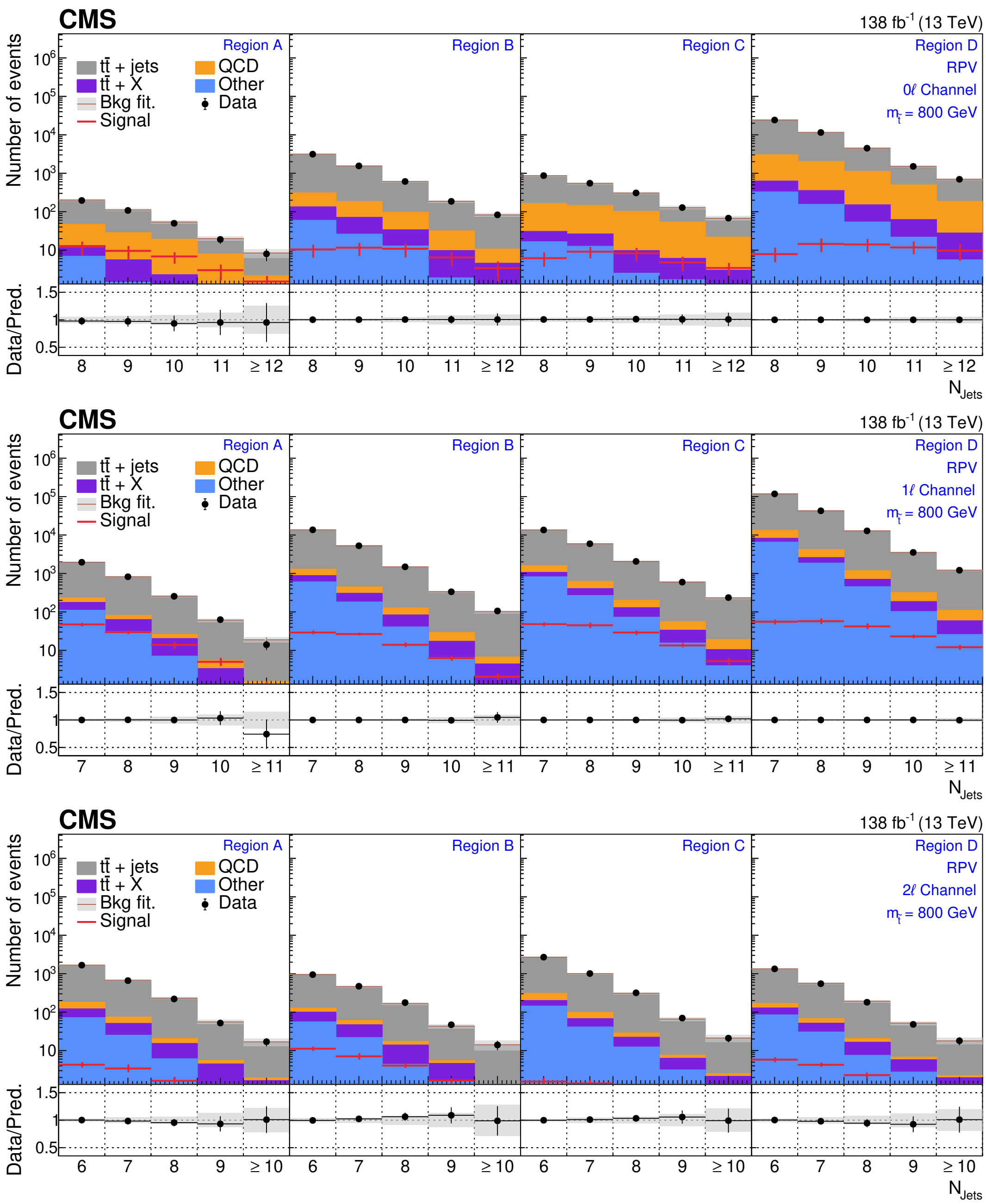

Figure A.2: The N_{jets} distributions from the background-only fits to data. Fits are run with the signal strength fixed to zero and all background process event yields are obtained from their fit predictions. The signal distribution overlaid corresponds to the RPV model with $m_{\tilde{t}} = 800\,\text{GeV}$. The graphs in the upper, middle, and lower rows correspond to the 0ℓ, 1ℓ, and 2ℓ channels, respectively. The four panels in each row show the N_{jets} distributions for the A, B, C, and D regions (left to right). The gray error band shows the combined statistical and systematic uncertainty from the background-only fit distributions.

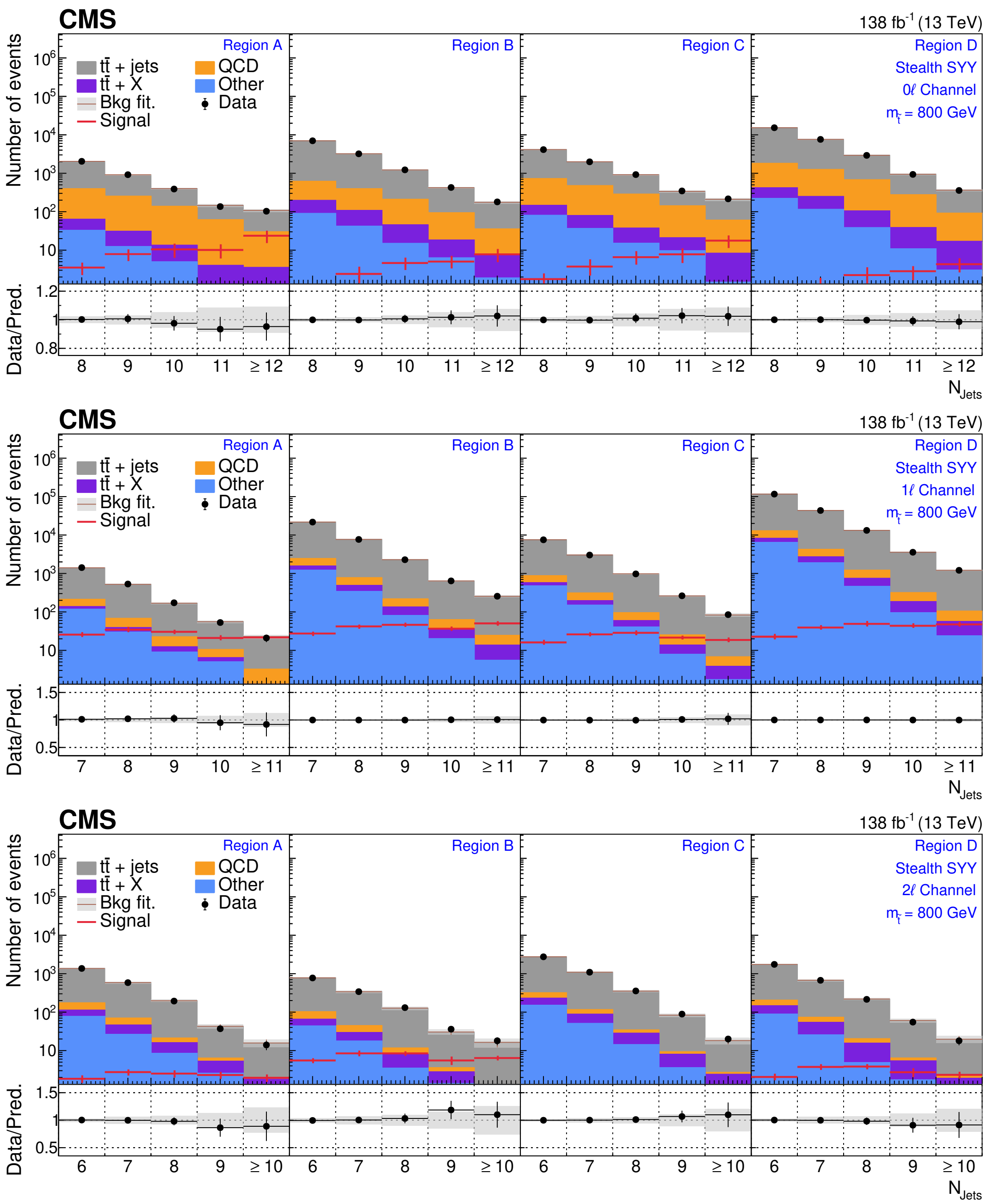

Figure A.3: The N_{jets} distributions from the background-only fits to data. Fits are run with the signal strength fixed to zero and all background process event yields are obtained from their fit predictions. The signal distribution overlaid corresponds to the stealth SY$\overline{\text{Y}}$ model with $m_{\tilde{t}} = 800\,\text{GeV}$. The graphs in the upper, middle, and lower rows correspond to the 0ℓ, 1ℓ, and 2ℓ channels, respectively. The four panels in each row show the N_{jets} distributions for the A, B, C, and D regions (left to right). The gray error band shows the combined statistical and systematic uncertainty from the background-only fit distributions.

B The CMS Collaboration

Yerevan Physics Institute, Yerevan, Armenia
V. Chekhovsky, A. Hayrapetyan, V. Makarenko, A. Tumasyan[1]

Institut für Hochenergiephysik, Vienna, Austria
W. Adam, J.W. Andrejkovic, L. Benato, T. Bergauer, S. Chatterjee, K. Damanakis, M. Dragicevic, P.S. Hussain, M. Jeitler[2], N. Krammer, A. Li, D. Liko, I. Mikulec, J. Schieck[2], R. Schöfbeck[2], D. Schwarz, M. Sonawane, W. Waltenberger, C.-E. Wulz[2]

Universiteit Antwerpen, Antwerpen, Belgium
T. Janssen, H. Kwon, T. Van Laer, P. Van Mechelen

Vrije Universiteit Brussel, Brussel, Belgium
N. Breugelmans, J. D'Hondt, S. Dansana, A. De Moor, M. Delcourt, F. Heyen, Y. Hong, S. Lowette, I. Makarenko, D. Müller, S. Tavernier, M. Tytgat[3], G.P. Van Onsem, S. Van Putte, D. Vannerom

Université Libre de Bruxelles, Bruxelles, Belgium
B. Bilin, B. Clerbaux, A.K. Das, I. De Bruyn, G. De Lentdecker, H. Evard, L. Favart, P. Gianneios, A. Khalilzadeh, F.A. Khan, K. Lee, A. Malara, M.A. Shahzad, L. Thomas, M. Vanden Bemden, C. Vander Velde, P. Vanlaer

Ghent University, Ghent, Belgium
M. De Coen, D. Dobur, G. Gokbulut, J. Knolle, L. Lambrecht, D. Marckx, K. Skovpen, N. Van Den Bossche, J. van der Linden, L. Wezenbeek

Université Catholique de Louvain, Louvain-la-Neuve, Belgium
S. Bein, A. Benecke, A. Bethani, G. Bruno, C. Caputo, J. De Favereau De Jeneret, C. Delaere, I.S. Donertas, A. Giammanco, A.O. Guzel, Sa. Jain, V. Lemaitre, J. Lidrych, P. Mastrapasqua, T.T. Tran, S. Turkcapar[4]

Centro Brasileiro de Pesquisas Fisicas, Rio de Janeiro, Brazil
G.A. Alves, E. Coelho, G. Correia Silva, C. Hensel, T. Menezes De Oliveira, C. Mora Herrera[5], P. Rebello Teles, M. Soeiro, E.J. Tonelli Manganote[6], A. Vilela Pereira[5]

Universidade do Estado do Rio de Janeiro, Rio de Janeiro, Brazil
W.L. Aldá Júnior, M. Barroso Ferreira Filho, H. Brandao Malbouisson, W. Carvalho, J. Chinellato[7], E.M. Da Costa, G.G. Da Silveira[8], D. De Jesus Damiao, S. Fonseca De Souza, R. Gomes De Souza, T. Laux Kuhn[8], M. Macedo, J. Martins, K. Mota Amarilo, L. Mundim, H. Nogima, J.P. Pinheiro, A. Santoro, A. Sznajder, M. Thiel

Universidade Estadual Paulista, Universidade Federal do ABC, São Paulo, Brazil
C.A. Bernardes[8], L. Calligaris, T.R. Fernandez Perez Tomei, E.M. Gregores, I. Maietto Silverio, P.G. Mercadante, S.F. Novaes, B. Orzari, Sandra S. Padula

Institute for Nuclear Research and Nuclear Energy, Bulgarian Academy of Sciences, Sofia, Bulgaria
A. Aleksandrov, G. Antchev, R. Hadjiiska, P. Iaydjiev, M. Misheva, M. Shopova, G. Sultanov

University of Sofia, Sofia, Bulgaria

A. Dimitrov, L. Litov, B. Pavlov, P. Petkov, A. Petrov, E. Shumka

Instituto De Alta Investigación, Universidad de Tarapacá, Casilla 7 D, Arica, Chile
S. Keshri, D. Laroze, S. Thakur

Beihang University, Beijing, China
T. Cheng, T. Javaid, L. Yuan

Department of Physics, Tsinghua University, Beijing, China
Z. Hu, Z. Liang, J. Liu

Institute of High Energy Physics, Beijing, China
G.M. Chen[9], H.S. Chen[9], M. Chen[9], F. Iemmi, C.H. Jiang, A. Kapoor[10], H. Liao, Z.-A. Liu[11], R. Sharma[12], J.N. Song[11], J. Tao, C. Wang[9], J. Wang, Z. Wang[9], H. Zhang, J. Zhao

State Key Laboratory of Nuclear Physics and Technology, Peking University, Beijing, China
A. Agapitos, Y. Ban, A. Carvalho Antunes De Oliveira, S. Deng, B. Guo, C. Jiang, A. Levin, C. Li, Q. Li, Y. Mao, S. Qian, S.J. Qian, X. Qin, X. Sun, D. Wang, H. Yang, Y. Zhao, C. Zhou

Guangdong Provincial Key Laboratory of Nuclear Science and Guangdong-Hong Kong Joint Laboratory of Quantum Matter, South China Normal University, Guangzhou, China
S. Yang

Sun Yat-Sen University, Guangzhou, China
Z. You

University of Science and Technology of China, Hefei, China
K. Jaffel, N. Lu

Nanjing Normal University, Nanjing, China
G. Bauer[13], B. Li[14], H. Wang, K. Yi[15], J. Zhang

Institute of Modern Physics and Key Laboratory of Nuclear Physics and Ion-beam Application (MOE) - Fudan University, Shanghai, China
Y. Li

Zhejiang University, Hangzhou, Zhejiang, China
Z. Lin, C. Lu, M. Xiao

Universidad de Los Andes, Bogota, Colombia
C. Avila, D.A. Barbosa Trujillo, A. Cabrera, C. Florez, J. Fraga, J.A. Reyes Vega

Universidad de Antioquia, Medellin, Colombia
J. Jaramillo, C. Rendón, M. Rodriguez, A.A. Ruales Barbosa, J.D. Ruiz Alvarez

University of Split, Faculty of Electrical Engineering, Mechanical Engineering and Naval Architecture, Split, Croatia
D. Giljanovic, N. Godinovic, D. Lelas, A. Sculac

University of Split, Faculty of Science, Split, Croatia
M. Kovac, A. Petkovic, T. Sculac

Institute Rudjer Boskovic, Zagreb, Croatia
P. Bargassa, V. Brigljevic, B.K. Chitroda, D. Ferencek, K. Jakovcic, A. Starodumov[16], T. Susa

University of Cyprus, Nicosia, Cyprus
A. Attikis, K. Christoforou, A. Hadjiagapiou, C. Leonidou, J. Mousa, C. Nicolaou, L. Paizanos, F. Ptochos, P.A. Razis, H. Rykaczewski, H. Saka, A. Stepennov

Charles University, Prague, Czech Republic
M. Finger, M. Finger Jr., A. Kveton

Escuela Politecnica Nacional, Quito, Ecuador
E. Ayala

Universidad San Francisco de Quito, Quito, Ecuador
E. Carrera Jarrin

Academy of Scientific Research and Technology of the Arab Republic of Egypt, Egyptian Network of High Energy Physics, Cairo, Egypt
A.A. Abdelalim[17,18], S. Elgammal[19], A. Ellithi Kamel[20]

Center for High Energy Physics (CHEP-FU), Fayoum University, El-Fayoum, Egypt
M. Abdullah Al-Mashad, M.A. Mahmoud

National Institute of Chemical Physics and Biophysics, Tallinn, Estonia
K. Ehataht, M. Kadastik, T. Lange, C. Nielsen, J. Pata, M. Raidal, L. Tani, C. Veelken

Department of Physics, University of Helsinki, Helsinki, Finland
K. Osterberg, M. Voutilainen

Helsinki Institute of Physics, Helsinki, Finland
N. Bin Norjoharuddeen, E. Brücken, F. Garcia, P. Inkaew, K.T.S. Kallonen, T. Lampén, K. Lassila-Perini, S. Lehti, T. Lindén, M. Myllymäki, M.m. Rantanen, J. Tuominiemi

Lappeenranta-Lahti University of Technology, Lappeenranta, Finland
H. Kirschenmann, P. Luukka, H. Petrow

IRFU, CEA, Université Paris-Saclay, Gif-sur-Yvette, France
M. Besancon, F. Couderc, M. Dejardin, D. Denegri, J.L. Faure, F. Ferri, S. Ganjour, P. Gras, G. Hamel de Monchenault, M. Kumar, V. Lohezic, J. Malcles, F. Orlandi, L. Portales, A. Rosowsky, M.Ö. Sahin, A. Savoy-Navarro[21], P. Simkina, M. Titov, M. Tornago

Laboratoire Leprince-Ringuet, CNRS/IN2P3, Ecole Polytechnique, Institut Polytechnique de Paris, Palaiseau, France
F. Beaudette, G. Boldrini, P. Busson, A. Cappati, C. Charlot, M. Chiusi, T.D. Cuisset, F. Damas, O. Davignon, A. De Wit, I.T. Ehle, B.A. Fontana Santos Alves, S. Ghosh, A. Gilbert, R. Granier de Cassagnac, A. Hakimi, B. Harikrishnan, L. Kalipoliti, G. Liu, M. Nguyen, S. Obraztsov, C. Ochando, R. Salerno, J.B. Sauvan, Y. Sirois, G. Sokmen, L. Urda Gómez, E. Vernazza, A. Zabi, A. Zghiche

Université de Strasbourg, CNRS, IPHC UMR 7178, Strasbourg, France
J.-L. Agram[22], J. Andrea, D. Apparu, D. Bloch, J.-M. Brom, E.C. Chabert, C. Collard, S. Falke, U. Goerlach, R. Haeberle, A.-C. Le Bihan, M. Meena, O. Poncet, G. Saha, M.A. Sessini, P. Van Hove, P. Vaucelle

Centre de Calcul de l'Institut National de Physique Nucleaire et de Physique des Particules,

CNRS/IN2P3, Villeurbanne, France
A. Di Florio

Institut de Physique des 2 Infinis de Lyon (IP2I), Villeurbanne, France
D. Amram, S. Beauceron, B. Blancon, G. Boudoul, N. Chanon, D. Contardo, P. Depasse, C. Dozen[23], H. El Mamouni, J. Fay, S. Gascon, M. Gouzevitch, C. Greenberg, G. Grenier, B. Ille, E. Jourd'huy, I.B. Laktineh, M. Lethuillier, L. Mirabito, S. Perries, A. Purohit, M. Vander Donckt, P. Verdier, J. Xiao

Georgian Technical University, Tbilisi, Georgia
I. Lomidze, T. Toriashvili[24], Z. Tsamalaidze[16]

RWTH Aachen University, I. Physikalisches Institut, Aachen, Germany
V. Botta, S. Consuegra Rodríguez, L. Feld, K. Klein, M. Lipinski, D. Meuser, A. Pauls, D. Pérez Adán, N. Röwert, M. Teroerde

RWTH Aachen University, III. Physikalisches Institut A, Aachen, Germany
S. Diekmann, A. Dodonova, N. Eich, D. Eliseev, F. Engelke, J. Erdmann, M. Erdmann, P. Fackeldey, B. Fischer, T. Hebbeker, K. Hoepfner, F. Ivone, A. Jung, M.y. Lee, F. Mausolf, M. Merschmeyer, A. Meyer, S. Mukherjee, D. Noll, F. Nowotny, A. Pozdnyakov, Y. Rath, W. Redjeb, F. Rehm, H. Reithler, V. Sarkisovi, A. Schmidt, C. Seth, A. Sharma, J.L. Spah, F. Torres Da Silva De Araujo[25], S. Wiedenbeck, S. Zaleski

RWTH Aachen University, III. Physikalisches Institut B, Aachen, Germany
C. Dziwok, G. Flügge, T. Kress, A. Nowack, O. Pooth, A. Stahl, T. Ziemons, A. Zotz

Deutsches Elektronen-Synchrotron, Hamburg, Germany
H. Aarup Petersen, M. Aldaya Martin, J. Alimena, S. Amoroso, Y. An, J. Bach, S. Baxter, M. Bayatmakou, H. Becerril Gonzalez, O. Behnke, A. Belvedere, F. Blekman[26], K. Borras[27], A. Campbell, A. Cardini, F. Colombina, M. De Silva, G. Eckerlin, D. Eckstein, L.I. Estevez Banos, E. Gallo[26], A. Geiser, V. Guglielmi, M. Guthoff, A. Hinzmann, L. Jeppe, B. Kaech, M. Kasemann, C. Kleinwort, R. Kogler, M. Komm, D. Krücker, W. Lange, D. Leyva Pernia, K. Lipka[28], W. Lohmann[29], F. Lorkowski, R. Mankel, I.-A. Melzer-Pellmann, M. Mendizabal Morentin, A.B. Meyer, G. Milella, K. Moral Figueroa, A. Mussgiller, L.P. Nair, J. Niedziela, A. Nürnberg, J. Park, E. Ranken, A. Raspereza, D. Rastorguev, J. Rübenach, L. Rygaard, M. Scham[30,27], S. Schnake[27], P. Schütze, C. Schwanenberger[26], D. Selivanova, K. Sharko, M. Shchedrolosiev, D. Stafford, F. Vazzoler, A. Ventura Barroso, R. Walsh, D. Wang, Q. Wang, K. Wichmann, L. Wiens[27], C. Wissing, Y. Yang, S. Zakharov, A. Zimermmane Castro Santos

University of Hamburg, Hamburg, Germany
A. Albrecht, S. Albrecht, M. Antonello, S. Bollweg, M. Bonanomi, P. Connor, K. El Morabit, Y. Fischer, E. Garutti, A. Grohsjean, J. Haller, D. Hundhausen, H.R. Jabusch, G. Kasieczka, P. Keicher, R. Klanner, W. Korcari, T. Kramer, C.c. Kuo, V. Kutzner, F. Labe, J. Lange, A. Lobanov, C. Matthies, L. Moureaux, M. Mrowietz, A. Nigamova, Y. Nissan, A. Paasch, K.J. Pena Rodriguez, T. Quadfasel, B. Raciti, M. Rieger, D. Savoiu, J. Schindler, P. Schleper, M. Schröder, J. Schwandt, M. Sommerhalder, H. Stadie, G. Steinbrück, A. Tews, B. Wiederspan, M. Wolf

Karlsruher Institut fuer Technologie, Karlsruhe, Germany
S. Brommer, E. Butz, T. Chwalek, A. Dierlamm, G.G. Dincer, U. Elicabuk, N. Faltermann, M. Giffels, A. Gottmann, F. Hartmann[31], R. Hofsaess, M. Horzela, U. Husemann, J. Kieseler, M. Klute, O. Lavoryk, J.M. Lawhorn, M. Link, A. Lintuluoto, S. Maier, S. Mitra, M. Mormile, Th. Müller, M. Neukum, M. Oh, E. Pfeffer, M. Presilla, G. Quast, K. Rabbertz, B. Regnery, N. Shadskiy, I. Shvetsov, H.J. Simonis, L. Sowa, L. Stockmeier, K. Tauqeer, M. Toms, B. Topko, N. Trevisani, R.F. Von Cube, M. Wassmer, S. Wieland, F. Wittig, R. Wolf, X. Zuo

Institute of Nuclear and Particle Physics (INPP), NCSR Demokritos, Aghia Paraskevi, Greece
G. Anagnostou, G. Daskalakis, A. Kyriakis, A. Papadopoulos[31], A. Stakia

National and Kapodistrian University of Athens, Athens, Greece
G. Melachroinos, Z. Painesis, I. Paraskevas, N. Saoulidou, K. Theofilatos, E. Tziaferi, K. Vellidis, I. Zisopoulos

National Technical University of Athens, Athens, Greece
G. Bakas, T. Chatzistavrou, G. Karapostoli, K. Kousouris, I. Papakrivopoulos, E. Siamarkou, G. Tsipolitis, A. Zacharopoulou

University of Ioánnina, Ioánnina, Greece
I. Bestintzanos, I. Evangelou, C. Foudas, C. Kamtsikis, P. Katsoulis, P. Kokkas, P.G. Kosmoglou Kioseoglou, N. Manthos, I. Papadopoulos, J. Strologas

HUN-REN Wigner Research Centre for Physics, Budapest, Hungary
C. Hajdu, D. Horvath[32,33], K. Márton, A.J. Rádl[34], F. Sikler, V. Veszpremi

MTA-ELTE Lendület CMS Particle and Nuclear Physics Group, Eötvös Loránd University, Budapest, Hungary
M. Csanád, K. Farkas, A. Fehérkuti[35], M.M.A. Gadallah[36], Á. Kadlecsik, P. Major, G. Pásztor, G.I. Veres

Faculty of Informatics, University of Debrecen, Debrecen, Hungary
B. Ujvari, G. Zilizi

HUN-REN ATOMKI - Institute of Nuclear Research, Debrecen, Hungary
G. Bencze, S. Czellar, J. Molnar, Z. Szillasi

Karoly Robert Campus, MATE Institute of Technology, Gyongyos, Hungary
T. Csorgo[35], F. Nemes[35], T. Novak

Panjab University, Chandigarh, India
S. Bansal, S.B. Beri, V. Bhatnagar, G. Chaudhary, S. Chauhan, N. Dhingra[37], A. Kaur, A. Kaur, H. Kaur, M. Kaur, S. Kumar, T. Sheokand, J.B. Singh, A. Singla

University of Delhi, Delhi, India
A. Bhardwaj, A. Chhetri, B.C. Choudhary, A. Kumar, A. Kumar, M. Naimuddin, K. Ranjan, M.K. Saini, S. Saumya

Saha Institute of Nuclear Physics, HBNI, Kolkata, India
S. Baradia, S. Barman[38], S. Bhattacharya, S. Das Gupta, S. Dutta, S. Dutta, S. Sarkar

Indian Institute of Technology Madras, Madras, India
M.M. Ameen, P.K. Behera, S.C. Behera, S. Chatterjee, G. Dash, P. Jana,

P. Kalbhor, S. Kamble, J.R. Komaragiri[39], D. Kumar[39], T. Mishra, B. Parida[40], P.R. Pujahari, N.R. Saha, A. Sharma, A.K. Sikdar, R.K. Singh, P. Verma, S. Verma, A. Vijay

Tata Institute of Fundamental Research-A, Mumbai, India
S. Dugad, G.B. Mohanty, M. Shelake, P. Suryadevara

Tata Institute of Fundamental Research-B, Mumbai, India
A. Bala, S. Banerjee, S. Bhowmik, R.M. Chatterjee, M. Guchait, Sh. Jain, A. Jaiswal, B.M. Joshi, S. Kumar, G. Majumder, K. Mazumdar, S. Parolia, A. Thachayath

National Institute of Science Education and Research, An OCC of Homi Bhabha National Institute, Bhubaneswar, Odisha, India
S. Bahinipati[41], C. Kar, D. Maity[42], P. Mal, K. Naskar[42], A. Nayak[42], S. Nayak, K. Pal, P. Sadangi, S.K. Swain, S. Varghese[42], D. Vats[42]

Indian Institute of Science Education and Research (IISER), Pune, India
S. Acharya[43], A. Alpana, S. Dube, B. Gomber[43], P. Hazarika, B. Kansal, A. Laha, B. Sahu[43], S. Sharma, K.Y. Vaish

Isfahan University of Technology, Isfahan, Iran
H. Bakhshiansohi[44], A. Jafari[45], M. Zeinali[46]

Institute for Research in Fundamental Sciences (IPM), Tehran, Iran
S. Bashiri, S. Chenarani[47], S.M. Etesami, Y. Hosseini, M. Khakzad, E. Khazaie, M. Mohammadi Najafabadi, S. Tizchang[48]

University College Dublin, Dublin, Ireland
M. Felcini, M. Grunewald

INFN Sezione di Bari[a], Università di Bari[b], Politecnico di Bari[c], Bari, Italy
M. Abbrescia[a,b], A. Colaleo[a,b], D. Creanza[a,c], B. D'Anzi[a,b], N. De Filippis[a,c], M. De Palma[a,b], W. Elmetenawee[a,b,17], N. Ferrara[a,b], L. Fiore[a], G. Iaselli[a,c], L. Longo[a], M. Louka[a,b], G. Maggi[a,c], M. Maggi[a], I. Margjeka[a], V. Mastrapasqua[a,b], S. My[a,b], S. Nuzzo[a,b], A. Pellecchia[a,b], A. Pompili[a,b], G. Pugliese[a,c], R. Radogna[a,b], D. Ramos[a], A. Ranieri[a], L. Silvestris[a], F.M. Simone[a,c], Ü. Sözbilir[a], A. Stamerra[a,b], D. Troiano[a,b], R. Venditti[a,b], P. Verwilligen[a], A. Zaza[a,b]

INFN Sezione di Bologna[a], Università di Bologna[b], Bologna, Italy
G. Abbiendi[a], C. Battilana[a,b], D. Bonacorsi[a,b], P. Capiluppi[a,b], A. Castro[†a,b], F.R. Cavallo[a], M. Cuffiani[a,b], G.M. Dallavalle[a], T. Diotalevi[a,b], F. Fabbri[a], A. Fanfani[a,b], D. Fasanella[a], P. Giacomelli[a], L. Giommi[a,b], C. Grandi[a], L. Guiducci[a,b], S. Lo Meo[a,49], M. Lorusso[a,b], L. Lunerti[a], S. Marcellini[a], G. Masetti[a], F.L. Navarria[a,b], G. Paggi[a,b], A. Perrotta[a], F. Primavera[a,b], A.M. Rossi[a,b], S. Rossi Tisbeni[a,b], T. Rovelli[a,b], G.P. Siroli[a,b]

INFN Sezione di Catania[a], Università di Catania[b], Catania, Italy
S. Costa[a,b,50], A. Di Mattia[a], A. Lapertosa[a], R. Potenza[a,b], A. Tricomi[a,b,50]

INFN Sezione di Firenze[a], Università di Firenze[b], Firenze, Italy
P. Assiouras[a], G. Barbagli[a], G. Bardelli[a,b], B. Camaiani[a,b], A. Cassese[a], R. Ceccarelli[a], V. Ciulli[a,b], C. Civinini[a], R. D'Alessandro[a,b], E. Focardi[a,b], T. Kello[a], G. Latino[a,b], P. Lenzi[a,b], M. Lizzo[a], M. Meschini[a], S. Paoletti[a], A. Papanastassiou[a,b], G. Sguazzoni[a], L. Viliani[a]

INFN Laboratori Nazionali di Frascati, Frascati, Italy
L. Benussi, S. Bianco, S. Meola[51], D. Piccolo

INFN Sezione di Genova[a], Università di Genova[b], Genova, Italy
M. Alves Gallo Pereira[a], F. Ferro[a], E. Robutti[a], S. Tosi[a,b]

INFN Sezione di Milano-Bicocca[a], Università di Milano-Bicocca[b], Milano, Italy
A. Benaglia[a], F. Brivio[a], F. Cetorelli[a,b], F. De Guio[a,b], M.E. Dinardo[a,b], P. Dini[a], S. Gennai[a], R. Gerosa[a,b], A. Ghezzi[a,b], P. Govoni[a,b], L. Guzzi[a], G. Lavizzari[a,b], M.T. Lucchini[a,b], M. Malberti[a], S. Malvezzi[a], A. Massironi[a], D. Menasce[a], L. Moroni[a], M. Paganoni[a,b], S. Palluotto[a,b], D. Pedrini[a], A. Perego[a,b], B.S. Pinolini[a], G. Pizzati[a,b], S. Ragazzi[a,b], T. Tabarelli de Fatis[a,b]

INFN Sezione di Napoli[a], Università di Napoli 'Federico II'[b], Napoli, Italy; Università della Basilicata[c], Potenza, Italy; Scuola Superiore Meridionale (SSM)[d], Napoli, Italy
S. Buontempo[a], A. Cagnotta[a,b], F. Carnevali[a,b], N. Cavallo[a,c], F. Fabozzi[a,c], A.O.M. Iorio[a,b], L. Lista[a,b,52], P. Paolucci[a,31], B. Rossi[a]

INFN Sezione di Padova[a], Università di Padova[b], Padova, Italy; Universita degli Studi di Cagliari[c], Cagliari, Italy
R. Ardino[a], P. Azzi[a], N. Bacchetta[a,53], D. Bisello[a,b], P. Bortignon[a], G. Bortolato[a,b], A. Bragagnolo[a,b], A.C.M. Bulla[a], R. Carlin[a,b], P. Checchia[a], T. Dorigo[a,54], F. Gasparini[a,b], U. Gasparini[a,b], S. Giorgetti[a], E. Lusiani[a], M. Margoni[a,b], A.T. Meneguzzo[a,b], M. Migliorini[a,b], M. Passaseo[a], J. Pazzini[a,b], P. Ronchese[a,b], R. Rossin[a,b], M. Sgaravatto[a], M. Tosi[a,b], A. Triossi[a,b], S. Ventura[a], M. Zanetti[a,b], P. Zotto[a,b], A. Zucchetta[a,b]

INFN Sezione di Pavia[a], Università di Pavia[b], Pavia, Italy
A. Braghieri[a], S. Calzaferri[a], D. Fiorina[a], P. Montagna[a,b], V. Re[a], C. Riccardi[a,b], P. Salvini[a], I. Vai[a,b], P. Vitulo[a,b]

INFN Sezione di Perugia[a], Università di Perugia[b], Perugia, Italy
S. Ajmal[a,b], M.E. Ascioti[a,b], G.M. Bilei[a], C. Carrivale[a,b], D. Ciangottini[a,b], L. Fanò[a,b], V. Mariani[a,b], M. Menichelli[a], F. Moscatelli[a,55], A. Rossi[a,b], A. Santocchia[a,b], D. Spiga[a], T. Tedeschi[a,b]

INFN Sezione di Pisa[a], Università di Pisa[b], Scuola Normale Superiore di Pisa[c], Pisa, Italy; Università di Siena[d], Siena, Italy
C. Aimè[a], C.A. Alexe[a,c], P. Asenov[a,b], P. Azzurri[a], G. Bagliesi[a], R. Bhattacharya[a], L. Bianchini[a,b], T. Boccali[a], E. Bossini[a], D. Bruschini[a,c], R. Castaldi[a], M.A. Ciocci[a,b], M. Cipriani[a,b], V. D'Amante[a,d], R. Dell'Orso[a], S. Donato[a], A. Giassi[a], F. Ligabue[a,c], A.C. Marini[a,b], D. Matos Figueiredo[a], A. Messineo[a,b], S. Mishra[a], V.K. Muraleedharan Nair Bindhu[a,b,42], M. Musich[a,b], S. Nandan[a], F. Palla[a], A. Rizzi[a,b], G. Rolandi[a,c], S. Roy Chowdhury[a], T. Sarkar[a], A. Scribano[a], P. Spagnolo[a], R. Tenchini[a], G. Tonelli[a,b], N. Turini[a,d], F. Vaselli[a,c], A. Venturi[a], P.G. Verdini[a]

INFN Sezione di Roma[a], Sapienza Università di Roma[b], Roma, Italy
P. Barria[a], C. Basile[a,b], F. Cavallari[a], L. Cunqueiro Mendez[a,b], D. Del Re[a,b], E. Di Marco[a,b], M. Diemoz[a], F. Errico[a,b], R. Gargiulo[a,b], E. Longo[a,b], L. Martikainen[a,b], J. Mijuskovic[a,b], G. Organtini[a,b], F. Pandolfi[a], R. Paramatti[a,b], C. Quaranta[a,b], S. Rahatlou[a,b], C. Rovelli[a], F. Santanastasio[a,b], L. Soffi[a], V. Vladimirov[a,b]

INFN Sezione di Torino[a], Università di Torino[b], Torino, Italy; Università del Piemonte Orientale[c], Novara, Italy
N. Amapane[a,b], R. Arcidiacono[a,c], S. Argiro[a,b], M. Arneodo[a,c], N. Bartosik[a], R. Bellan[a,b], C. Biino[a], C. Borca[a,b], N. Cartiglia[a], M. Costa[a,b], R. Covarelli[a,b], N. Demaria[a], L. Finco[a], M. Grippo[a,b], B. Kiani[a,b], F. Legger[a], F. Luongo[a,b], C. Mariotti[a], L. Markovic[a,b], S. Maselli[a], A. Mecca[a,b], L. Menzio[a,b], P. Meridiani[a], E. Migliore[a,b], M. Monteno[a], R. Mulargia[a], M.M. Obertino[a,b], G. Ortona[a], L. Pacher[a,b], N. Pastrone[a], M. Pelliccioni[a], M. Ruspa[a,c], F. Siviero[a,b], V. Sola[a,b], A. Solano[a,b], A. Staiano[a], C. Tarricone[a,b], D. Trocino[a], G. Umoret[a,b], R. White[a,b]

INFN Sezione di Trieste[a], Università di Trieste[b], Trieste, Italy
J. Babbar[a,b], S. Belforte[a], V. Candelise[a,b], M. Casarsa[a], F. Cossutti[a], K. De Leo[a], G. Della Ricca[a,b]

Kyungpook National University, Daegu, Korea
S. Dogra, J. Hong, J. Kim, D. Lee, H. Lee, S.W. Lee, C.S. Moon, Y.D. Oh, M.S. Ryu, S. Sekmen, B. Tae, Y.C. Yang

Department of Mathematics and Physics - GWNU, Gangneung, Korea
M.S. Kim

Chonnam National University, Institute for Universe and Elementary Particles, Kwangju, Korea
G. Bak, P. Gwak, H. Kim, D.H. Moon

Hanyang University, Seoul, Korea
E. Asilar, J. Choi[56], D. Kim, T.J. Kim, J.A. Merlin, Y. Ryou

Korea University, Seoul, Korea
S. Choi, S. Han, B. Hong, K. Lee, K.S. Lee, S. Lee, J. Yoo

Kyung Hee University, Department of Physics, Seoul, Korea
J. Goh, S. Yang

Sejong University, Seoul, Korea
Y. Kang, H. S. Kim, Y. Kim, S. Lee

Seoul National University, Seoul, Korea
J. Almond, J.H. Bhyun, J. Choi, J. Choi, W. Jun, J. Kim, Y.W. Kim, S. Ko, H. Lee, J. Lee, J. Lee, B.H. Oh, S.B. Oh, H. Seo, U.K. Yang, I. Yoon

University of Seoul, Seoul, Korea
W. Jang, D.Y. Kang, S. Kim, B. Ko, J.S.H. Lee, Y. Lee, I.C. Park, Y. Roh, I.J. Watson

Yonsei University, Department of Physics, Seoul, Korea
S. Ha, K. Hwang, B. Kim, H.D. Yoo

Sungkyunkwan University, Suwon, Korea
M. Choi, M.R. Kim, H. Lee, Y. Lee, I. Yu

College of Engineering and Technology, American University of the Middle East (AUM), Dasman, Kuwait
T. Beyrouthy, Y. Gharbia

Kuwait University - College of Science - Department of Physics, Safat, Kuwait
F. Alazemi

Riga Technical University, Riga, Latvia
K. Dreimanis, A. Gaile, C. Munoz Diaz, D. Osite, G. Pikurs, A. Potrebko, M. Seidel, D. Sidiropoulos Kontos

University of Latvia (LU), Riga, Latvia
N.R. Strautnieks

Vilnius University, Vilnius, Lithuania
M. Ambrozas, A. Juodagalvis, A. Rinkevicius, G. Tamulaitis

National Centre for Particle Physics, Universiti Malaya, Kuala Lumpur, Malaysia
I. Yusuff[57], Z. Zolkapli

Universidad de Sonora (UNISON), Hermosillo, Mexico
J.F. Benitez, A. Castaneda Hernandez, H.A. Encinas Acosta, L.G. Gallegos Maríñez, M. León Coello, J.A. Murillo Quijada, A. Sehrawat, L. Valencia Palomo

Centro de Investigacion y de Estudios Avanzados del IPN, Mexico City, Mexico
G. Ayala, H. Castilla-Valdez, H. Crotte Ledesma, E. De La Cruz-Burelo, I. Heredia-De La Cruz[58], R. Lopez-Fernandez, J. Mejia Guisao, C.A. Mondragon Herrera, A. Sánchez Hernández

Universidad Iberoamericana, Mexico City, Mexico
C. Oropeza Barrera, D.L. Ramirez Guadarrama, M. Ramírez García

Benemerita Universidad Autonoma de Puebla, Puebla, Mexico
I. Bautista, F.E. Neri Huerta, I. Pedraza, H.A. Salazar Ibarguen, C. Uribe Estrada

University of Montenegro, Podgorica, Montenegro
I. Bubanja, N. Raicevic

University of Canterbury, Christchurch, New Zealand
P.H. Butler

National Centre for Physics, Quaid-I-Azam University, Islamabad, Pakistan
A. Ahmad, M.I. Asghar, A. Awais, M.I.M. Awan, H.R. Hoorani, W.A. Khan

AGH University of Krakow, Krakow, Poland
V. Avati, A. Bellora, L. Forthomme, L. Grzanka, M. Malawski, K. Piotrzkowski

National Centre for Nuclear Research, Swierk, Poland
H. Bialkowska, M. Bluj, M. Górski, M. Kazana, M. Szleper, P. Zalewski

Institute of Experimental Physics, Faculty of Physics, University of Warsaw, Warsaw, Poland
K. Bunkowski, K. Doroba, A. Kalinowski, M. Konecki, J. Krolikowski, A. Muhammad

Warsaw University of Technology, Warsaw, Poland
P. Fokow, K. Pozniak, W. Zabolotny

Laboratório de Instrumentação e Física Experimental de Partículas, Lisboa, Portugal
M. Araujo, D. Bastos, C. Beirão Da Cruz E Silva, A. Boletti, M. Bozzo, T. Camporesi, G. Da Molin, P. Faccioli, M. Gallinaro, J. Hollar, N. Leonardo, G.B. Marozzo, A. Petrilli, M. Pisano, J. Seixas, J. Varela, J.W. Wulff

Faculty of Physics, University of Belgrade, Belgrade, Serbia
P. Adzic, P. Milenovic

VINCA Institute of Nuclear Sciences, University of Belgrade, Belgrade, Serbia
D. Devetak, M. Dordevic, J. Milosevic, L. Nadderd, V. Rekovic, M. Stojanovic

Centro de Investigaciones Energéticas Medioambientales y Tecnológicas (CIEMAT), Madrid, Spain
J. Alcaraz Maestre, Cristina F. Bedoya, J.A. Brochero Cifuentes, Oliver M. Carretero, M. Cepeda, M. Cerrada, N. Colino, B. De La Cruz, A. Delgado Peris, A. Escalante Del Valle, D. Fernández Del Val, J.P. Fernández Ramos, J. Flix, M.C. Fouz, O. Gonzalez Lopez, S. Goy Lopez, J.M. Hernandez, M.I. Josa, J. Llorente Merino, C. Martin Perez, E. Martin Viscasillas, D. Moran, C. M. Morcillo Perez, Á. Navarro Tobar, C. Perez Dengra, A. Pérez-Calero Yzquierdo, J. Puerta Pelayo, I. Redondo, J. Sastre, J. Vazquez Escobar

Universidad Autónoma de Madrid, Madrid, Spain
J.F. de Trocóniz

Universidad de Oviedo, Instituto Universitario de Ciencias y Tecnologías Espaciales de Asturias (ICTEA), Oviedo, Spain
B. Alvarez Gonzalez, J. Cuevas, J. Fernandez Menendez, S. Folgueras, I. Gonzalez Caballero, P. Leguina, E. Palencia Cortezon, J. Prado Pico, V. Rodríguez Bouza, A. Soto Rodríguez, A. Trapote, C. Vico Villalba, P. Vischia

Instituto de Física de Cantabria (IFCA), CSIC-Universidad de Cantabria, Santander, Spain
S. Blanco Fernández, I.J. Cabrillo, A. Calderon, J. Duarte Campderros, M. Fernandez, G. Gomez, C. Lasaosa García, R. Lopez Ruiz, C. Martinez Rivero, P. Martinez Ruiz del Arbol, F. Matorras, P. Matorras Cuevas, E. Navarrete Ramos, J. Piedra Gomez, L. Scodellaro, I. Vila, J.M. Vizan Garcia

University of Colombo, Colombo, Sri Lanka
B. Kailasapathy[59], D.D.C. Wickramarathna

University of Ruhuna, Department of Physics, Matara, Sri Lanka
W.G.D. Dharmaratna[60], K. Liyanage, N. Perera

CERN, European Organization for Nuclear Research, Geneva, Switzerland
D. Abbaneo, C. Amendola, E. Auffray, G. Auzinger, J. Baechler, D. Barney, A. Bermúdez Martínez, M. Bianco, A.A. Bin Anuar, A. Bocci, L. Borgonovi, C. Botta, E. Brondolin, C.E. Brown, C. Caillol, G. Cerminara, N. Chernyavskaya, D. d'Enterria, A. Dabrowski, A. David, A. De Roeck, M.M. Defranchis, M. Deile, M. Dobson, G. Franzoni, W. Funk, S. Giani, D. Gigi, K. Gill, F. Glege, M. Glowacki, J. Hegeman, J.K. Heikkilä, B. Huber, V. Innocente, T. James, P. Janot, O. Kaluzinska, O. Karacheban[29], G. Karathanasis, S. Laurila, P. Lecoq, E. Leutgeb, C. Lourenço, M. Magherini, L. Malgeri, M. Mannelli, M. Matthewman, A. Mehta, F. Meijers, S. Mersi, E. Meschi, V. Milosevic, F. Monti, F. Moortgat, M. Mulders, I. Neutelings, S. Orfanelli, F. Pantaleo, G. Petrucciani, A. Pfeiffer, M. Pierini, H. Qu, D. Rabady, B. Ribeiro Lopes, F. Riti, M. Rovere, H. Sakulin, R. Salvatico, S. Sanchez Cruz, S. Scarfi, C. Schwick, M. Selvaggi, A. Sharma, K. Shchelina, P. Silva, P. Sphicas[61], A.G. Stahl Leiton, A. Steen, S. Summers, D. Treille, P. Tropea, D. Walter, J. Wanczyk[62], J. Wang, S. Wuchterl, P. Zehetner, P. Zejdl, W.D. Zeuner

PSI Center for Neutron and Muon Sciences, Villigen, Switzerland
T. Bevilacqua[63], L. Caminada[63], A. Ebrahimi, W. Erdmann, R. Horisberger,

Q. Ingram, H.C. Kaestli, D. Kotlinski, C. Lange, M. Missiroli[63], L. Noehte[63], T. Rohe, A. Samalan

ETH Zurich - Institute for Particle Physics and Astrophysics (IPA), Zurich, Switzerland
T.K. Aarrestad, M. Backhaus, G. Bonomelli, A. Calandri, C. Cazzaniga, K. Datta, P. De Bryas Dexmiers D'archiac[62], A. De Cosa, G. Dissertori, M. Dittmar, M. Donegà, F. Eble, M. Galli, K. Gedia, F. Glessgen, C. Grab, N. Härringer, T.G. Harte, D. Hits, W. Lustermann, A.-M. Lyon, R.A. Manzoni, M. Marchegiani, L. Marchese, A. Mascellani[62], F. Nessi-Tedaldi, F. Pauss, V. Perovic, S. Pigazzini, B. Ristic, R. Seidita, J. Steggemann[62], A. Tarabini, D. Valsecchi, R. Wallny

Universität Zürich, Zurich, Switzerland
C. Amsler[64], P. Bärtschi, M.F. Canelli, K. Cormier, M. Huwiler, W. Jin, A. Jofrehei, B. Kilminster, S. Leontsinis, S.P. Liechti, A. Macchiolo, P. Meiring, F. Meng, J. Motta, A. Reimers, P. Robmann, M. Senger, E. Shokr, F. Stäger, R. Tramontano

National Central University, Chung-Li, Taiwan
C. Adloff[65], D. Bhowmik, C.M. Kuo, W. Lin, P.K. Rout, P.C. Tiwari[39]

National Taiwan University (NTU), Taipei, Taiwan
L. Ceard, K.F. Chen, Z.g. Chen, A. De Iorio, W.-S. Hou, T.h. Hsu, Y.w. Kao, S. Karmakar, G. Kole, Y.y. Li, R.-S. Lu, E. Paganis, X.f. Su, J. Thomas-Wilsker, L.s. Tsai, D. Tsionou, H.y. Wu, E. Yazgan

High Energy Physics Research Unit, Department of Physics, Faculty of Science, Chulalongkorn University, Bangkok, Thailand
C. Asawatangtrakuldee, N. Srimanobhas, V. Wachirapusitanand

Tunis El Manar University, Tunis, Tunisia
Y. Maghrbi

Çukurova University, Physics Department, Science and Art Faculty, Adana, Turkey
D. Agyel, F. Boran, F. Dolek, I. Dumanoglu[66], E. Eskut, Y. Guler[67], E. Gurpinar Guler[67], C. Isik, O. Kara, A. Kayis Topaksu, Y. Komurcu, G. Onengut, K. Ozdemir[68], A. Polatoz, B. Tali[69], U.G. Tok, E. Uslan, I.S. Zorbakir

Middle East Technical University, Physics Department, Ankara, Turkey
M. Yalvac[70]

Bogazici University, Istanbul, Turkey
B. Akgun, I.O. Atakisi, E. Gülmez, M. Kaya[71], O. Kaya[72], S. Tekten[73]

Istanbul Technical University, Istanbul, Turkey
A. Cakir, K. Cankocak[66,74], S. Sen[75]

Istanbul University, Istanbul, Turkey
O. Aydilek[76], B. Hacisahinoglu, I. Hos[77], B. Kaynak, S. Ozkorucuklu, O. Potok, H. Sert, C. Simsek, C. Zorbilmez

Yildiz Technical University, Istanbul, Turkey
S. Cerci, B. Isildak[78], D. Sunar Cerci, T. Yetkin

Institute for Scintillation Materials of National Academy of Science of Ukraine, Kharkiv, Ukraine
A. Boyaryntsev, B. Grynyov

National Science Centre, Kharkiv Institute of Physics and Technology, Kharkiv, Ukraine
L. Levchuk

University of Bristol, Bristol, United Kingdom
D. Anthony, J.J. Brooke, A. Bundock, F. Bury, E. Clement, D. Cussans, H. Flacher, J. Goldstein, H.F. Heath, M.-L. Holmberg, L. Kreczko, S. Paramesvaran, L. Robertshaw, V.J. Smith, K. Walkingshaw Pass

Rutherford Appleton Laboratory, Didcot, United Kingdom
A.H. Ball, K.W. Bell, A. Belyaev[79], C. Brew, R.M. Brown, D.J.A. Cockerill, C. Cooke, A. Elliot, K.V. Ellis, K. Harder, S. Harper, J. Linacre, K. Manolopoulos, D.M. Newbold, E. Olaiya, D. Petyt, T. Reis, A.R. Sahasransu, G. Salvi, T. Schuh, C.H. Shepherd-Themistocleous, I.R. Tomalin, K.C. Whalen, T. Williams

Imperial College, London, United Kingdom
I. Andreou, R. Bainbridge, P. Bloch, O. Buchmuller, C.A. Carrillo Montoya, G.S. Chahal[80], D. Colling, J.S. Dancu, I. Das, P. Dauncey, G. Davies, M. Della Negra, S. Fayer, G. Fedi, G. Hall, A. Howard, G. Iles, C.R. Knight, P. Krueper, J. Langford, K.H. Law, J. León Holgado, L. Lyons, A.-M. Magnan, B. Maier, S. Mallios, M. Mieskolainen, J. Nash[81], M. Pesaresi, P.B. Pradeep, B.C. Radburn-Smith, A. Richards, A. Rose, K. Savva, C. Seez, R. Shukla, A. Tapper, K. Uchida, G.P. Uttley, T. Virdee[31], M. Vojinovic, N. Wardle, D. Winterbottom

Brunel University, Uxbridge, United Kingdom
J.E. Cole, A. Khan, P. Kyberd, I.D. Reid

Baylor University, Waco, Texas, USA
S. Abdullin, A. Brinkerhoff, E. Collins, M.R. Darwish, J. Dittmann, K. Hatakeyama, V. Hegde, J. Hiltbrand, B. McMaster, J. Samudio, S. Sawant, C. Sutantawibul, J. Wilson

Catholic University of America, Washington, DC, USA
R. Bartek, A. Dominguez, A.E. Simsek, S.S. Yu

The University of Alabama, Tuscaloosa, Alabama, USA
B. Bam, A. Buchot Perraguin, R. Chudasama, S.I. Cooper, C. Crovella, S.V. Gleyzer, E. Pearson, C.U. Perez, P. Rumerio[82], E. Usai, R. Yi

Boston University, Boston, Massachusetts, USA
A. Akpinar, C. Cosby, G. De Castro, Z. Demiragli, C. Erice, C. Fangmeier, C. Fernandez Madrazo, E. Fontanesi, D. Gastler, F. Golf, S. Jeon, J. O'cain, I. Reed, J. Rohlf, K. Salyer, D. Sperka, D. Spitzbart, I. Suarez, A. Tsatsos, A.G. Zecchinelli

Brown University, Providence, Rhode Island, USA
G. Barone, G. Benelli, D. Cutts, L. Gouskos, M. Hadley, U. Heintz, K.W. Ho, J.M. Hogan[83], T. Kwon, G. Landsberg, K.T. Lau, J. Luo, S. Mondal, T. Russell, S. Sagir[84], X. Shen, M. Stamenkovic, N. Venkatasubramanian

University of California, Davis, Davis, California, USA
S. Abbott, B. Barton, C. Brainerd, R. Breedon, H. Cai, M. Calderon De La Barca Sanchez, M. Chertok, M. Citron, J. Conway, P.T. Cox, R. Erbacher, F. Jensen, O. Kukral, G. Mocellin, M. Mulhearn, S. Ostrom,

W. Wei, S. Yoo, F. Zhang

University of California, Los Angeles, California, USA
K. Adamidis, M. Bachtis, D. Campos, R. Cousins, A. Datta, G. Flores Avila, J. Hauser, M. Ignatenko, M.A. Iqbal, T. Lam, Y.f. Lo, E. Manca, A. Nunez Del Prado, D. Saltzberg, V. Valuev

University of California, Riverside, Riverside, California, USA
R. Clare, J.W. Gary, G. Hanson

University of California, San Diego, La Jolla, California, USA
A. Aportela, A. Arora, J.G. Branson, S. Cittolin, S. Cooperstein, D. Diaz, J. Duarte, L. Giannini, Y. Gu, J. Guiang, R. Kansal, V. Krutelyov, R. Lee, J. Letts, M. Masciovecchio, F. Mokhtar, S. Mukherjee, M. Pieri, D. Primosch, M. Quinnan, V. Sharma, M. Tadel, E. Vourliotis, F. Würthwein, Y. Xiang, A. Yagil

University of California, Santa Barbara - Department of Physics, Santa Barbara, California, USA
A. Barzdukas, L. Brennan, C. Campagnari, K. Downham, C. Grieco, M.M. Hussain, J. Incandela, J. Kim, A.J. Li, P. Masterson, H. Mei, J. Richman, S.N. Santpur, U. Sarica, R. Schmitz, F. Setti, J. Sheplock, D. Stuart, T.Á. Vámi, X. Yan, D. Zhang

California Institute of Technology, Pasadena, California, USA
S. Bhattacharya, A. Bornheim, O. Cerri, J. Mao, H.B. Newman, G. Reales Gutiérrez, M. Spiropulu, J.R. Vlimant, C. Wang, S. Xie, R.Y. Zhu

Carnegie Mellon University, Pittsburgh, Pennsylvania, USA
J. Alison, S. An, P. Bryant, M. Cremonesi, V. Dutta, T. Ferguson, T.A. Gómez Espinosa, A. Harilal, A. Kallil Tharayil, C. Liu, T. Mudholkar, S. Murthy, P. Palit, K. Park, M. Paulini, A. Roberts, A. Sanchez, W. Terrill

University of Colorado Boulder, Boulder, Colorado, USA
J.P. Cumalat, W.T. Ford, A. Hart, A. Hassani, N. Manganelli, J. Pearkes, C. Savard, N. Schonbeck, K. Stenson, K.A. Ulmer, S.R. Wagner, N. Zipper, D. Zuolo

Cornell University, Ithaca, New York, USA
J. Alexander, X. Chen, D.J. Cranshaw, J. Dickinson, J. Fan, X. Fan, S. Hogan, P. Kotamnives, J. Monroy, M. Oshiro, J.R. Patterson, M. Reid, A. Ryd, J. Thom, P. Wittich, R. Zou

Fermi National Accelerator Laboratory, Batavia, Illinois, USA
M. Albrow, M. Alyari, O. Amram, G. Apollinari, A. Apresyan, L.A.T. Bauerdick, D. Berry, J. Berryhill, P.C. Bhat, K. Burkett, J.N. Butler, A. Canepa, G.B. Cerati, H.W.K. Cheung, F. Chlebana, G. Cummings, I. Dutta, V.D. Elvira, J. Freeman, A. Gandrakota, Z. Gecse, L. Gray, D. Green, A. Grummer, S. Grünendahl, D. Guerrero, O. Gutsche, R.M. Harris, T.C. Herwig, J. Hirschauer, B. Jayatilaka, S. Jindariani, M. Johnson, U. Joshi, T. Klijnsma, B. Klima, K.H.M. Kwok, S. Lammel, C. Lee, D. Lincoln, R. Lipton, T. Liu, K. Maeshima, D. Mason, P. McBride, P. Merkel, S. Mrenna, S. Nahn, J. Ngadiuba, D. Noonan, S. Norberg, V. Papadimitriou, N. Pastika, K. Pedro, C. Pena[85], F. Ravera, A. Reinsvold Hall[86], L. Ristori, M. Safdari, E. Sexton-Kennedy, N. Smith,

A. Soha, L. Spiegel, S. Stoynev, J. Strait, L. Taylor, S. Tkaczyk, N.V. Tran, L. Uplegger, E.W. Vaandering, I. Zoi

University of Florida, Gainesville, Florida, USA
C. Aruta, P. Avery, D. Bourilkov, P. Chang, V. Cherepanov, R.D. Field, C. Huh, E. Koenig, M. Kolosova, J. Konigsberg, A. Korytov, K. Matchev, N. Menendez, G. Mitselmakher, K. Mohrman, A. Muthirakalayil Madhu, N. Rawal, S. Rosenzweig, Y. Takahashi, J. Wang

Florida State University, Tallahassee, Florida, USA
T. Adams, A. Al Kadhim, A. Askew, S. Bower, R. Hashmi, R.S. Kim, S. Kim, T. Kolberg, G. Martinez, H. Prosper, P.R. Prova, M. Wulansatiti, R. Yohay, J. Zhang

Florida Institute of Technology, Melbourne, Florida, USA
B. Alsufyani, S. Butalla, S. Das, T. Elkafrawy[87], M. Hohlmann, E. Yanes

University of Illinois Chicago, Chicago, Illinois, USA
M.R. Adams, A. Baty, C. Bennett, R. Cavanaugh, R. Escobar Franco, O. Evdokimov, C.E. Gerber, M. Hawksworth, A. Hingrajiya, D.J. Hofman, J.h. Lee, D. S. Lemos, C. Mills, S. Nanda, G. Oh, B. Ozek, D. Pilipovic, R. Pradhan, E. Prifti, T. Roy, S. Rudrabhatla, N. Singh, M.B. Tonjes, N. Varelas, M.A. Wadud, Z. Ye, J. Yoo

The University of Iowa, Iowa City, Iowa, USA
M. Alhusseini, D. Blend, K. Dilsiz[88], L. Emediato, G. Karaman, O.K. Köseyan, J.-P. Merlo, A. Mestvirishvili[89], O. Neogi, H. Ogul[90], Y. Onel, A. Penzo, C. Snyder, E. Tiras[91]

Johns Hopkins University, Baltimore, Maryland, USA
B. Blumenfeld, L. Corcodilos, J. Davis, A.V. Gritsan, L. Kang, S. Kyriacou, P. Maksimovic, M. Roguljic, J. Roskes, S. Sekhar, M. Swartz

The University of Kansas, Lawrence, Kansas, USA
A. Abreu, L.F. Alcerro Alcerro, J. Anguiano, S. Arteaga Escatel, P. Baringer, A. Bean, Z. Flowers, D. Grove, J. King, G. Krintiras, M. Lazarovits, C. Le Mahieu, J. Marquez, M. Murray, M. Nickel, M. Pitt, S. Popescu[92], C. Rogan, C. Royon, S. Sanders, C. Smith, G. Wilson

Kansas State University, Manhattan, Kansas, USA
B. Allmond, R. Gujju Gurunadha, A. Ivanov, K. Kaadze, Y. Maravin, J. Natoli, D. Roy, G. Sorrentino

University of Maryland, College Park, Maryland, USA
A. Baden, A. Belloni, J. Bistany-riebman, Y.M. Chen, S.C. Eno, N.J. Hadley, S. Jabeen, R.G. Kellogg, T. Koeth, B. Kronheim, Y. Lai, S. Lascio, A.C. Mignerey, S. Nabili, C. Palmer, C. Papageorgakis, M.M. Paranjpe, E. Popova[93], A. Shevelev, L. Wang, L. Zhang

Massachusetts Institute of Technology, Cambridge, Massachusetts, USA
C. Baldenegro Barrera, J. Bendavid, S. Bright-Thonney, I.A. Cali, P.c. Chou, M. D'Alfonso, J. Eysermans, C. Freer, G. Gomez-Ceballos, M. Goncharov, G. Grosso, P. Harris, D. Hoang, D. Kovalskyi, J. Krupa, L. Lavezzo, Y.-J. Lee, K. Long, C. Mcginn, A. Novak, M.I. Park, C. Paus, C. Reissel, C. Roland, G. Roland, S. Rothman, G.S.F. Stephans, Z. Wang, B. Wyslouch, T. J. Yang

University of Minnesota, Minneapolis, Minnesota, USA
B. Crossman, C. Kapsiak, M. Krohn, D. Mahon, J. Mans, B. Marzocchi, M. Revering, R. Rusack, R. Saradhy, N. Strobbe

University of Nebraska-Lincoln, Lincoln, Nebraska, USA
K. Bloom, D.R. Claes, G. Haza, J. Hossain, C. Joo, I. Kravchenko, A. Rohilla, J.E. Siado, W. Tabb, A. Vagnerini, A. Wightman, F. Yan, D. Yu

State University of New York at Buffalo, Buffalo, New York, USA
H. Bandyopadhyay, L. Hay, H.w. Hsia, I. Iashvili, A. Kalogeropoulos, A. Kharchilava, M. Morris, D. Nguyen, S. Rappoccio, H. Rejeb Sfar, A. Williams, P. Young

Northeastern University, Boston, Massachusetts, USA
G. Alverson, E. Barberis, J. Bonilla, B. Bylsma, M. Campana, J. Dervan, Y. Haddad, Y. Han, I. Israr, A. Krishna, P. Levchenko, J. Li, M. Lu, R. Mccarthy, D.M. Morse, V. Nguyen, T. Orimoto, A. Parker, L. Skinnari, E. Tsai, D. Wood

Northwestern University, Evanston, Illinois, USA
S. Dittmer, K.A. Hahn, D. Li, Y. Liu, M. Mcginnis, Y. Miao, D.G. Monk, M.H. Schmitt, A. Taliercio, M. Velasco

University of Notre Dame, Notre Dame, Indiana, USA
G. Agarwal, R. Band, R. Bucci, S. Castells, A. Das, R. Goldouzian, M. Hildreth, K. Hurtado Anampa, T. Ivanov, C. Jessop, K. Lannon, J. Lawrence, N. Loukas, L. Lutton, J. Mariano, N. Marinelli, I. Mcalister, T. McCauley, C. Mcgrady, C. Moore, Y. Musienko[16], H. Nelson, M. Osherson, A. Piccinelli, R. Ruchti, A. Townsend, Y. Wan, M. Wayne, H. Yockey, M. Zarucki, L. Zygala

The Ohio State University, Columbus, Ohio, USA
A. Basnet, M. Carrigan, L.S. Durkin, C. Hill, M. Joyce, M. Nunez Ornelas, K. Wei, D.A. Wenzl, B.L. Winer, B. R. Yates

Princeton University, Princeton, New Jersey, USA
H. Bouchamaoui, K. Coldham, P. Das, G. Dezoort, P. Elmer, A. Frankenthal, B. Greenberg, N. Haubrich, K. Kennedy, G. Kopp, S. Kwan, D. Lange, A. Loeliger, D. Marlow, I. Ojalvo, J. Olsen, F. Simpson, D. Stickland, C. Tully, L.H. Vage

University of Puerto Rico, Mayaguez, Puerto Rico, USA
S. Malik, R. Sharma

Purdue University, West Lafayette, Indiana, USA
A.S. Bakshi, S. Chandra, R. Chawla, A. Gu, L. Gutay, M. Jones, A.W. Jung, A.M. Koshy, M. Liu, G. Negro, N. Neumeister, G. Paspalaki, S. Piperov, V. Scheurer, J.F. Schulte, A. K. Virdi, F. Wang, A. Wildridge, W. Xie, Y. Yao

Purdue University Northwest, Hammond, Indiana, USA
J. Dolen, N. Parashar, A. Pathak

Rice University, Houston, Texas, USA
D. Acosta, A. Agrawal, T. Carnahan, K.M. Ecklund, P.J. Fernández Manteca, S. Freed, P. Gardner, F.J.M. Geurts, I. Krommydas, W. Li, J. Lin, O. Miguel Colin, B.P. Padley, R. Redjimi, J. Rotter, E. Yigitbasi, Y. Zhang

University of Rochester, Rochester, New York, USA
A. Bodek, P. de Barbaro, R. Demina, J.L. Dulemba, A. Garcia-Bellido, O. Hindrichs, A. Khukhunaishvili, N. Parmar, P. Parygin[93], R. Taus

Rutgers, The State University of New Jersey, Piscataway, New Jersey, USA
B. Chiarito, J.P. Chou, S.V. Clark, D. Gadkari, Y. Gershtein, E. Halkiadakis, M. Heindl, C. Houghton, D. Jaroslawski, S. Konstantinou, I. Laflotte, A. Lath, R. Montalvo, K. Nash, J. Reichert, P. Saha, S. Salur, S. Schnetzer, S. Somalwar, R. Stone, S.A. Thayil, S. Thomas, J. Vora

University of Tennessee, Knoxville, Tennessee, USA
D. Ally, A.G. Delannoy, S. Fiorendi, S. Higginbotham, T. Holmes, A.R. Kanuganti, N. Karunarathna, L. Lee, E. Nibigira, S. Spanier

Texas A&M University, College Station, Texas, USA
D. Aebi, M. Ahmad, T. Akhter, K. Androsov[62], O. Bouhali[94], R. Eusebi, J. Gilmore, T. Huang, T. Kamon[95], H. Kim, S. Luo, R. Mueller, D. Overton, A. Safonov

Texas Tech University, Lubbock, Texas, USA
N. Akchurin, J. Damgov, Y. Feng, N. Gogate, Y. Kazhykarim, K. Lamichhane, S.W. Lee, C. Madrid, A. Mankel, T. Peltola, I. Volobouev

Vanderbilt University, Nashville, Tennessee, USA
E. Appelt, Y. Chen, S. Greene, A. Gurrola, W. Johns, R. Kunnawalkam Elayavalli, A. Melo, D. Rathjens, F. Romeo, P. Sheldon, S. Tuo, J. Velkovska, J. Viinikainen

University of Virginia, Charlottesville, Virginia, USA
B. Cardwell, H. Chung, B. Cox, J. Hakala, R. Hirosky, A. Ledovskoy, C. Mantilla, C. Neu, C. Ramón Álvarez

Wayne State University, Detroit, Michigan, USA
S. Bhattacharya, P.E. Karchin

University of Wisconsin - Madison, Madison, Wisconsin, USA
A. Aravind, S. Banerjee, K. Black, T. Bose, E. Chavez, S. Dasu, P. Everaerts, C. Galloni, H. He, M. Herndon, A. Herve, C.K. Koraka, A. Lanaro, R. Loveless, J. Madhusudanan Sreekala, A. Mallampalli, A. Mohammadi, S. Mondal, G. Parida, L. Pétré, D. Pinna, A. Savin, V. Shang, V. Sharma, W.H. Smith, D. Teague, H.F. Tsoi, W. Vetens, A. Warden

Authors affiliated with an international laboratory covered by a cooperation agreement with CERN
S. Afanasiev, V. Alexakhin, D. Budkouski, I. Golutvin[†], I. Gorbunov, V. Karjavine, O. Kodolova[96], V. Korenkov, A. Lanev, A. Malakhov, V. Matveev[97], A. Nikitenko[98,96], V. Palichik, V. Perelygin, M. Savina, V. Shalaev, S. Shmatov, S. Shulha, V. Smirnov, O. Teryaev, N. Voytishin, B.S. Yuldashev[†99], A. Zarubin, I. Zhizhin

Authors affiliated with an institute formerly covered by a cooperation agreement with CERN
G. Gavrilov, V. Golovtcov, Y. Ivanov, V. Kim[97], V. Murzin, V. Oreshkin, D. Sosnov, V. Sulimov, L. Uvarov, A. Vorobyev[†], Yu. Andreev, A. Dermenev, S. Gninenko, N. Golubev, A. Karneyeu, D. Kirpichnikov, M. Kirsanov, N. Krasnikov, I. Tlisova, A. Toropin, T. Aushev, K. Ivanov, V. Gavrilov, N. Ly-

chkovskaya, V. Popov, A. Zhokin, M. Chadeeva[97], R. Chistov[97], S. Polikarpov[97], V. Andreev, M. Azarkin, M. Kirakosyan, A. Terkulov, E. Boos, V. Bunichev, M. Dubinin[85], L. Dudko, A. Gribushin, V. Klyukhin, M. Perfilov, V. Savrin, P. Volkov, G. Vorotnikov, V. Blinov[97], T. Dimova[97], A. Kozyrev[97], O. Radchenko[97], Y. Skovpen[97], V. Kachanov, S. Slabospitskii, A. Uzunian, A. Babaev, V. Borshch, D. Druzhkin

†: Deceased
[1]Also at Yerevan State University, Yerevan, Armenia
[2]Also at TU Wien, Vienna, Austria
[3]Also at Ghent University, Ghent, Belgium
[4]Also at Çukurova University, Physics Department, Science and Art Faculty, Adana, Turkey
[5]Also at Universidade do Estado do Rio de Janeiro, Rio de Janeiro, Brazil
[6]Also at FACAMP - Faculdades de Campinas, Sao Paulo, Brazil
[7]Also at Universidade Estadual de Campinas, Campinas, Brazil
[8]Also at Federal University of Rio Grande do Sul, Porto Alegre, Brazil
[9]Also at University of Chinese Academy of Sciences, Beijing, China
[10]Also at China Center of Advanced Science and Technology, Beijing, China
[11]Also at University of Chinese Academy of Sciences, Beijing, China
[12]Also at China Spallation Neutron Source, Guangdong, China
[13]Now at Henan Normal University, Xinxiang, China
[14]Also at University of Shanghai for Science and Technology, Shanghai, China
[15]Now at The University of Iowa, Iowa City, Iowa, USA
[16]Also at an institute formerly covered by a cooperation agreement with CERN
[17]Also at Helwan University, Cairo, Egypt
[18]Now at Zewail City of Science and Technology, Zewail, Egypt
[19]Now at British University in Egypt, Cairo, Egypt
[20]Now at Cairo University, Cairo, Egypt
[21]Also at Purdue University, West Lafayette, Indiana, USA
[22]Also at Université de Haute Alsace, Mulhouse, France
[23]Also at Istinye University, Istanbul, Turkey
[24]Also at Tbilisi State University, Tbilisi, Georgia
[25]Also at The University of the State of Amazonas, Manaus, Brazil
[26]Also at University of Hamburg, Hamburg, Germany
[27]Also at RWTH Aachen University, III. Physikalisches Institut A, Aachen, Germany
[28]Also at Bergische University Wuppertal (BUW), Wuppertal, Germany
[29]Also at Brandenburg University of Technology, Cottbus, Germany
[30]Also at Forschungszentrum Jülich, Juelich, Germany
[31]Also at CERN, European Organization for Nuclear Research, Geneva, Switzerland
[32]Also at HUN-REN ATOMKI - Institute of Nuclear Research, Debrecen, Hungary
[33]Now at Universitatea Babes-Bolyai - Facultatea de Fizica, Cluj-Napoca, Romania
[34]Also at MTA-ELTE Lendület CMS Particle and Nuclear Physics Group, Eötvös Loránd University, Budapest, Hungary
[35]Also at HUN-REN Wigner Research Centre for Physics, Budapest, Hungary
[36]Also at Physics Department, Faculty of Science, Assiut University, Assiut, Egypt
[37]Also at Punjab Agricultural University, Ludhiana, India
[38]Also at University of Visva-Bharati, Santiniketan, India
[39]Also at Indian Institute of Science (IISc), Bangalore, India
[40]Also at Amity University Uttar Pradesh, Noida, India
[41]Also at IIT Bhubaneswar, Bhubaneswar, India

[42]Also at Institute of Physics, Bhubaneswar, India
[43]Also at University of Hyderabad, Hyderabad, India
[44]Also at Deutsches Elektronen-Synchrotron, Hamburg, Germany
[45]Also at Isfahan University of Technology, Isfahan, Iran
[46]Also at Sharif University of Technology, Tehran, Iran
[47]Also at Department of Physics, University of Science and Technology of Mazandaran, Behshahr, Iran
[48]Also at Department of Physics, Faculty of Science, Arak University, ARAK, Iran
[49]Also at Italian National Agency for New Technologies, Energy and Sustainable Economic Development, Bologna, Italy
[50]Also at Centro Siciliano di Fisica Nucleare e di Struttura Della Materia, Catania, Italy
[51]Also at Università degli Studi Guglielmo Marconi, Roma, Italy
[52]Also at Scuola Superiore Meridionale, Università di Napoli 'Federico II', Napoli, Italy
[53]Also at Fermi National Accelerator Laboratory, Batavia, Illinois, USA
[54]Also at Lulea University of Technology, Lulea, Sweden
[55]Also at Consiglio Nazionale delle Ricerche - Istituto Officina dei Materiali, Perugia, Italy
[56]Also at Institut de Physique des 2 Infinis de Lyon (IP2I), Villeurbanne, France
[57]Also at Department of Applied Physics, Faculty of Science and Technology, Universiti Kebangsaan Malaysia, Bangi, Malaysia
[58]Also at Consejo Nacional de Ciencia y Tecnología, Mexico City, Mexico
[59]Also at Trincomalee Campus, Eastern University, Sri Lanka, Nilaveli, Sri Lanka
[60]Also at Saegis Campus, Nugegoda, Sri Lanka
[61]Also at National and Kapodistrian University of Athens, Athens, Greece
[62]Also at Ecole Polytechnique Fédérale Lausanne, Lausanne, Switzerland
[63]Also at Universität Zürich, Zurich, Switzerland
[64]Also at Stefan Meyer Institute for Subatomic Physics, Vienna, Austria
[65]Also at Laboratoire d'Annecy-le-Vieux de Physique des Particules, IN2P3-CNRS, Annecy-le-Vieux, France
[66]Also at Near East University, Research Center of Experimental Health Science, Mersin, Turkey
[67]Also at Konya Technical University, Konya, Turkey
[68]Also at Izmir Bakircay University, Izmir, Turkey
[69]Also at Adiyaman University, Adiyaman, Turkey
[70]Also at Bozok Universitetesi Rektörlügü, Yozgat, Turkey
[71]Also at Marmara University, Istanbul, Turkey
[72]Also at Milli Savunma University, Istanbul, Turkey
[73]Also at Kafkas University, Kars, Turkey
[74]Now at Istanbul Okan University, Istanbul, Turkey
[75]Also at Hacettepe University, Ankara, Turkey
[76]Also at Erzincan Binali Yildirim University, Erzincan, Turkey
[77]Also at Istanbul University - Cerrahpasa, Faculty of Engineering, Istanbul, Turkey
[78]Also at Yildiz Technical University, Istanbul, Turkey
[79]Also at School of Physics and Astronomy, University of Southampton, Southampton, United Kingdom
[80]Also at IPPP Durham University, Durham, United Kingdom
[81]Also at Monash University, Faculty of Science, Clayton, Australia
[82]Also at Università di Torino, Torino, Italy
[83]Also at Bethel University, St. Paul, Minnesota, USA
[84]Also at Karamanoğlu Mehmetbey University, Karaman, Turkey

[85]Also at California Institute of Technology, Pasadena, California, USA
[86]Also at United States Naval Academy, Annapolis, Maryland, USA
[87]Also at Ain Shams University, Cairo, Egypt
[88]Also at Bingol University, Bingol, Turkey
[89]Also at Georgian Technical University, Tbilisi, Georgia
[90]Also at Sinop University, Sinop, Turkey
[91]Also at Erciyes University, Kayseri, Turkey
[92]Also at Horia Hulubei National Institute of Physics and Nuclear Engineering (IFIN-HH), Bucharest, Romania
[93]Now at another institute formerly covered by a cooperation agreement with CERN
[94]Also at Texas A&M University at Qatar, Doha, Qatar
[95]Also at Kyungpook National University, Daegu, Korea
[96]Also at Yerevan Physics Institute, Yerevan, Armenia
[97]Also at another institute formerly covered by a cooperation agreement with CERN
[98]Also at Imperial College, London, United Kingdom
[99]Also at Institute of Nuclear Physics of the Uzbekistan Academy of Sciences, Tashkent, Uzbekistan